Copy 6
RM A9I27

NACA RM A9I27

NACA

RESEARCH MEMORANDUM

AERODYNAMIC STUDY OF A WING-FUSELAGE COMBINATION EMPLOYING A WING SWEPT BACK 63°.- EFFECTS AT SUBSONIC SPEEDS OF A CONSTANT-CHORD ELEVON ON A WING CAMBERED AND TWISTED FOR A UNIFORM LOAD AT A LIFT COEFFICIENT OF 0.25

By J. Lloyd Jones and Fred A. Demele

Ames Aeronautical Laboratory
Moffett Field, Calif.

NATIONAL ADVISORY COMMITTEE
FOR AERONAUTICS

WASHINGTON
December 5, 1949

NACA RM A9I27

NATIONAL ADVISORY COMMITTEE FOR AERONAUTICS

RESEARCH MEMORANDUM

AERODYNAMIC STUDY OF A WING-FUSELAGE COMBINATION EMPLOYING A WING SWEPT BACK 63°.- EFFECTS AT SUBSONIC SPEEDS OF A CONSTANT-CHORD ELEVON ON A WING CAMBERED AND TWISTED FOR A UNIFORM LOAD AT A LIFT COEFFICIENT OF 0.25

By J. Lloyd Jones and Fred A. Demele

SUMMARY

A cambered and twisted wing having a leading edge swept back 63° and equipped with constant-chord elevons was tested in combination with a slender fuselage to determine the longitudinal and lateral control afforded by the elevons from a Mach number of 0.20 up to a Mach number of 0.93. The tests were performed at a Reynolds number of 2.0 million. Data are presented showing lift, drag, pitching-moment, and rolling-moment characteristics of the model for various elevon deflections, and hinge-moment characteristics of the elevon. Data from the tests have been applied to the calculation of the longitudinal-stability and -control characteristics of a hypothetical airplane geometrically similar to the model.

With the elevons undeflected, the model was longitudinally unstable about the one-quarter point of the wing mean aerodynamic chord at lift coefficients above about 0.50. The elevons had sufficient pitching-moment and rolling-moment effectiveness for all lift coefficients at which the model was longitudinally stable. At low speeds, the lift coefficient at which static longitudinal instability occurred was decreased by increasing negative elevon deflection. Increasing the Mach number increased the pitching-moment effectiveness at lift coefficients above 0.20, but reduced the rolling-moment effectiveness of the elevons.

INTRODUCTION

A coordinated research program has been undertaken by the Ames Aeronautical Laboratory for an aerodynamic investigation of a wing-fuselage combination employing a wing having the leading edge swept back 63°. Aerodynamic characteristics of such a wing with no camber or twist have been presented in references 1, 2, 3, and 4. Reference 1 includes low-speed data on the effectiveness of a constant-chord elevon, and reference 2 reports the Mach number and Reynolds number effects on the effectiveness of the same elevon.

Camber and twist have been incorporated in the wing in an effort to improve the flow near the wing tips where, as was evident from early investigations, loss of lift occurred even at very low angles of attack. Aerodynamic characteristics of such a wing, cambered and twisted to support a uniform distribution of lift over its surface at a lift coefficient of 0.25 and a Mach number of 1.5, have been presented in references 5 and 6.

This report presents the results of tests in the Ames 12-foot pressure wind tunnel of the effectiveness and hinge moments of constant-chord elevons at Mach numbers ranging up to 0.93. The elevons extended over the outer 50 percent of the span of the cambered and twisted wing, which is described in reference 6, and had the same plan form as the elevons on the model used for the tests reported in references 1 and 2.

NOTATION

a speed of sound, feet per second

b wing span measured perpendicular to plane of symmetry, feet

c local chord measured parallel to plane of symmetry, feet

$\bar{c}$ wing mean aerodynamic chord $\left(\dfrac{\int_0^{b/2} c^2\, dy}{\int_0^{b/2} c\, dy}\right)$, feet

C_D drag coefficient $\left(\dfrac{\text{drag}}{qS}\right)$

C_h hinge-moment coefficient $\left(\dfrac{\text{hinge moment}}{2q \times \text{area moment of elevon about elevon hinge axis}}\right)$

C_L lift coefficient $\left(\dfrac{\text{lift}}{qS}\right)$

C_l rolling-moment coefficient $\left(\dfrac{\text{rolling moment}}{qSb}\right)$

C_{l_p} damping-moment coefficient in roll; the rate of change of rolling-moment coefficient C_l with wing-tip helix angle $pb/2V$, per radian

C_m pitching-moment coefficient about the one-quarter point of the wing mean aerodynamic chord $\left(\dfrac{\text{pitching moment}}{qS\bar{c}}\right)$.

C_{m_δ}* $\left[\frac{(C_m)_{\delta=-4^\circ} - (C_m)_{\delta=0^\circ}}{-4}\right]$

H	hinge moment, foot-pounds
M	Mach number $\left(\frac{V}{a}\right)$
n	normal acceleration factor
p	angular velocity in roll, radians per second
q	dynamic pressure $\left(\frac{1}{2}\rho V^2\right)$, pounds per square foot
R	Reynolds number $\left(\frac{\rho V \bar{c}}{\mu}\right)$
S	wing area, square feet
V	free-stream velocity, feet per second
V_v	sinking speed, feet per second
V_G	gliding speed, miles per hour
y	lateral ordinate, feet
α	angle of attack of root chord line, degrees
α_t	angle of twist with reference to root chord (positive for washin), degrees
α_u	angle of attack of root chord line, uncorrected for tunnel-wall interference, degrees
δ	elevon deflection measured in planes perpendicular to the elevon hinge axes (positive downward), degrees
δ_u	elevon deflection uncorrected for angular distortion due to load, degrees
δ_{L_u}	left elevon deflection uncorrected for angular distortion due to load,degrees
δ_{R_u}	right elevon deflection uncorrected for angular distortion due to load,degrees
δ_T	arithmetic sum of positive and negative elevon deflections, degrees

[redacted]

δ_{T_u} arithmetic sum of positive and negative elevon deflections uncorrected for angular distortion due to load, degrees

μ coefficient of viscosity of air, slugs per foot-second

ρ mass density of air, slugs per cubic foot

MODEL AND APPARATUS

The model used in this investigation was the one used in the tests reported in reference 6. Photographs of the model are presented in figure 1 and dimensions are given in figures 2 and 3.

The wing had a leading-edge sweepback of 63°, a taper ratio of 0.25, and an aspect ratio of 3.5. The streamwise airfoil sections had the NACA 64A005 thickness distribution combined with a = 1 mean camber lines. The wing, as developed theoretically by the method given in reference 7, was cambered and twisted to support a uniform distribution of lift over its surface at a lift coefficient of 0.25 and a Mach number of 1.5. To provide for twisting of the wing under aerodynamic loads, the model wing was constructed with less twist than was indicated by theory, as is described in reference 6.

The elevons were of constant chord and extended over the outer 50 percent of the span. Each elevon was supported by three hinges and was restrained near the inner extremity. The ratio of elevon chord to wing chord was 1 to 4 at the wing midsemispan. The elevons had radius noses with no aerodynamic balance. The nose gaps were approximately 3/64 inch and were unsealed. These large gaps were necessary to permit the desired angular deflection since the elevons had considerable spanwise curvature. Hinge moments were measured by means of a wire-resistance strain gage mounted on the restraining member of the elevon on the left-hand wing.

The model was sting mounted, and the angle of attack was continuously controllable from a remote station during wind-tunnel operation. Forces and moments acting upon the model were measured by means of a wire-resistance strain-gage balance enclosed by the fuselage.

TESTS

Lift, drag, pitching-moment, rolling-moment, and elevon-hinge-moment data have been obtained throughout an angle-of-attack range of −8° to +19°. This range was more limited at the larger elevon deflections and higher Mach numbers where vibration of either the model or its support or wind-tunnel power limits were critical. All tests were made at an angle of sideslip of 0°. The elevons were deflected negatively for longitudinal control and differentially for lateral control as given in the following table:

[redacted]

Elevon deflection angles			
Longitudinal-control data		Lateral-control data	
δ_{L_u} (deg)	δ_{R_u} (deg)	δ_{L_u} (deg)	δ_{R_u} (deg)
0	0	0	0
-5	-5	10	-10
-10	-10	20	-20
-15	-15	30	-30
-20	-20	-	-
-25	-25	-	-

The tests were performed at several Mach numbers ranging from 0.20 to 0.93 at a constant Reynolds number of 2.0 million.

CORRECTIONS

The data have been corrected for the effects of tunnel-wall interference, constriction due to the tunnel walls, base pressure, and static tares due to the weight of the model. No correction has been applied to account for the change of elevon deflection under load upon the force and moment coefficients except when presented as functions of elevon angle. The angle of attack of the model was measured visually by means of a cathetometer; hence, no corrections were necessary to account for deflection of the support equipment. Precision of the force and moment measurements obtained from the strain-gage balance has been discussed in reference 6.

Tunnel-Wall Interference

Corrections to the data to account for induced tunnel-wall interference have been determined by the method of Glauert (reference 8). Since the ratio of model span to tunnel diameter was small, the total corrections were small, and no account was taken of sweepback or of the differential flap deflections. The following corrections were added:

$$\Delta\alpha = 0.26\ C_L$$

$$\Delta C_D = 0.0046\ C_L^2$$

No correction was applied to the pitching moment.

Constriction

The constriction effects of the tunnel walls have been evaluated by the method of reference 9. No modification of this method has been made to account for the effects of sweepback. The magnitude of the corrections applied to the Mach number and to the dynamic pressure is illustrated by the following table:

Corrected Mach number	Uncorrected Mach number	$\frac{q, \text{ corrected}}{q, \text{ uncorrected}}$
0.930	0.919	1.012
.890	.884	1.007
.800	.798	1.003
.600	.599	1.002
.200	.200	1.001

Base Pressure

The pressure on the base of the model fuselage was measured and, in an effort to correct for support interference, the drag data were corrected to correspond to a base pressure equal to the static pressure of the free stream. The base-pressure correction to the drag was less than 5 percent for Mach numbers up to 0.75, and increased to approximately 20 percent at a Mach number of 0.93. The base-pressure correction reduced the drag.

Tares

There were no tares due to direct air forces on the model-support equipment, since the balance was within the model. Corrections were made for the change in static tares due to angle of attack.

RESULTS AND DISCUSSION

Longitudinal Characteristics

Elevon effectiveness and hinge moments.- Angle of attack, drag coefficient, and pitching-moment coefficient as functions of lift coefficient, and hinge-moment coefficient as a function of angle of attack are presented in figures 4 to 8, inclusive, for various elevon deflections for Mach numbers ranging from 0.20 to 0.93. The angle of attack for zero lift became more positive as the elevon was deflected upward and the minimum drag coefficient was increased considerably by negative elevon deflections greater than -5°.

[redacted]

The elevon had sufficient pitching-moment effectiveness to provide longitudinal balance at all test Mach numbers for all positive lift coefficients at which the model had static longitudinal stability. The positive lift coefficient at which the loss of static longitudinal stability occurred (about 0.5) was reduced with increasing negative elevon deflection at a Mach number of 0.20, and generally increased with negative elevon deflection greater than -5° at higher Mach numbers. A slight forward movement of the aerodynamic center at zero lift was noted as the elevon was deflected negatively, and the movement became larger at the higher Mach numbers.

The change of elevon hinge moment with angle of attack was nearly uniform between angles of attack of -1° and $+8^\circ$ at a Mach number of 0.20 and between -1° and $+6^\circ$ for all other test Mach numbers. The variation of hinge-moment coefficient with angle of attack became considerably larger at angles of attack beyond these ranges. The sharply defined change of slope of the hinge-moment curves occurred coincidentally with the rearward movement of the aerodynamic center noted in the pitching-moment data.

The variations of lift coefficient, pitching-moment coefficient, and hinge-moment coefficient with elevon deflection are presented in figure 9 for constant angles of attack at several Mach numbers. The pitching-moment effectiveness of the elevons was generally maintained throughout the entire range of elevon deflection.

The effect of Mach number on the pitching-moment effectiveness of the elevons and on the lift coefficient for longitudinal balance is shown in figure 10. The pitching-moment effectiveness was nearly independent of Mach number at lift coefficients below 0.20 over the test range of Mach numbers. The effectiveness $-C_{m_\delta}{}^*$ increased with increasing Mach number at lift coefficients greater than 0.20. The lift coefficient for longitudinal balance was essentially unaffected by compressibility up to a Mach number of 0.80 for negative elevon deflection of 10° or less, and it is indicated that for negative deflections of 5° or less the lift coefficient for longitudinal balance was little affected by compressibility throughout the entire test range of Mach numbers.

Lift-drag ratio.- Figure 11 presents the variation of lift-drag ratio with lift coefficient for various elevon deflections at several Mach numbers. The highest maximum lift-drag ratio occurred with an elevon deflection of -5°, which suggests that increasing the wing twist would result in a higher maximum lift-drag ratio for the wing with the elevons undeflected.

Lateral Control

Elevon effectiveness and hinge moments.- Rolling-moment coefficients due to elevon deflection are presented in figure 12 as a function

cf angle of attack for differential elevon deflections of ± 10°, ± 20°, and ± 30° at Mach numbers ranging from 0.20 to 0.93. Also presented in figure 12 are elevon-hinge-moment coefficients for the left elevon only (the deflection of which was positive) over the same range of elevon deflections and Mach numbers. These data indicate that the effectiveness of the elevons in producing rolling moment was maintained throughout the test range of angle of attack and Mach number. The effectiveness was nearly constant at angles of attack between −1° and +8° for a Mach number of 0.20, and between −1° and +6° for the higher Mach numbers. The angles of attack at which the rolling-moment effectiveness of the elevons began to decrease rapidly coincide with those at which the rearward movement of the aerodynamic center is noted in the pitching-moment data. The variation of elevon-hinge-moment coefficient with angle of attack remained fairly uniform over the same angle-of-attack range for which the maximum rolling-moment effectiveness was maintained. At angles of attack just beyond these ranges the variation of hinge-moment coefficient with angle of attack became considerably greater, and at the larger positive angles of attack became erratic.

The variation of rolling-moment coefficient with total elevon deflection (the arithmetic sum of the positive and negative deflections) was smooth to the largest deflection, as may be seen in figure 13. Increasing the Mach number from 0.20 to 0.93 reduced the effectiveness by roughly 10 percent for an angle of attack of 6° and by about 25 percent for an angle of attack of 10° at the largest elevon deflection $\delta_u = \pm 30°$. The effect of Mach number on the rolling-moment effectiveness of the elevons is summarized in figure 14 for angles of attack of 0° and 4°. The rolling moment produced by a given elevon deflection was generally reduced slightly with increasing Mach number, the effect becoming greater with increasing deflections.

Helix angle.— On the basis of the methods presented in reference 10, helix angles generated by the wing tip in a steady roll have been calculated utilizing the data of figure 12. For the purposes of the calculations no torsional deflection and 0° of sideslip were assumed. Values of the damping-moment coefficient C_{l_p}, calculated by the method of reference 11, varied from −0.226 at a Mach number of 0.20 to −0.231 at a Mach number of 0.93.

The variation of the predicted wing-tip helix angle with total elevon deflection δ_T is presented in figure 15 for various Mach numbers at a lift coefficient of 0.20. As anticipated from the decrease in rolling effectiveness above an angle of attack of 8°, calculations of $pb/2V$ at a lift coefficient of 0.40 indicated a considerable decrease from its value at a lift coefficient of 0.20. No such calculations are presented herein, however, since above a Mach number of 0.20 the test angle-of-attack range was insufficient to evaluate corrections to the rolling-moment coefficient in roll. The variation of $pb/2V$ with δ_T was fairly linear throughout the range of elevon deflections considered.

Increasing Mach number generally reduced the helix angle. While the predicted wing-tip helix angle is large enough to insure high rolling velocities, it must be emphasized that the present calculations are for a rigid wing and that deflection of the wing could cause serious reductions in the magnitude of the rolling velocity.

Longitudinal Control of a Hypothetical Airplane

Data from the tests have been used in the calculation of the stability, maneuverability, elevon hinge moments, and power-off sinking speed of a hypothetical tailless airplane, geometrically similar to the model tested. Dimensions of the airplane were assumed to be as follows:

Wing span, feet	50
Wing area, square feet	714.3
Total elevon area, square feet	89.14

The center of gravity was assumed to be at 25 percent of the mean aerodynamic chord, and a wing loading of 40 pounds per square foot was assumed.

Figure 16 presents elevon hinge moment, elevon deflection, and lift coefficient as functions of Mach number calculated for the airplane in level flight and as affected by normal acceleration at an altitude of 25,000 feet. The variation of elevon deflection with Mach number and with normal acceleration factor was smooth and uniform. A very large variation of hinge moment with Mach number is noted for normal acceleration factors greater than 1.0. For unaccelerated flight ($n = 1.0$) increasing Mach number would require a gradually increasing push force up to a Mach number of 0.90. For a normal acceleration factor of 2.0, increasing Mach number is accompanied by a gradually decreasing push force. For constant-speed maneuvers with varying normal acceleration there are large and erratic changes in the hinge moment.

Power-off sinking speed, elevon deflection for balance, elevon hinge moment, and angle of attack are presented in figure 17 as functions of power-off gliding speed for sea-level operation. (Data at a Mach number of 0.20 were used in calculating the performance parameters shown in this figure.) The minimum power-off sinking speed is 22 feet per second and it occurs at a forward speed of approximately 215 miles per hour. The variation of elevon deflection required for longitudinal balance with gliding speed was stable for gliding speeds greater than 180 miles per hour. No computations are shown for gliding speeds less than 180 miles per hour, since the data indicated that the airplane would be longitudinally unstable at the required lift coefficients.

SUMMARY OF RESULTS

Tests have been made of a cambered and twisted wing with the leading edge swept back 63° in combination with a slender fuselage. The wing was equipped with constant-chord elevons extending over the outer 50 percent of the span. The tests were conducted at a Reynolds number of 2.0 million and at Mach numbers ranging from 0.20 to 0.93. The following results were obtained:

1. At low speed (M = 0.20) negative elevon deflections reduced the lift coefficient at which the loss of static longitudinal stability occurred, while at higher Mach numbers this lift coefficient generally increased with negative elevon deflections greater than -5°. (With the elevons undeflected the loss of static longitudinal stability generally occurred at a lift coefficient of about 0.5.)

2. There was little effect of compressibility on the pitching-moment effectiveness of the elevons at lift coefficients of 0.20 or less. At higher lift coefficients the effectiveness increased with increasing Mach number.

3. The effectiveness of the elevons in producing rolling moment was reduced slightly with increasing Mach number. The effectiveness was nearly constant at angles of attack between -1° and +8° for a Mach number of 0.20 and between -1° and +6° for the higher Mach numbers.

Ames Aeronautical Laboratory,
National Advisory Committee for Aeronautics,
Moffett Field, California.

REFERENCES

1. Hopkins, Edward J.: Aerodynamic Study of a Wing-Fuselage Combination Employing a Wing Swept Back 63°.- Effects of Split Flaps, Elevons, and Leading-Edge Devices at Low Speed. NACA RM A9C21, 1949.

2. Reynolds, Robert M., and Smith, Donald W.: Aerodynamic Study of a Wing-Fuselage Combination Employing a Wing Swept Back 63°.- Subsonic Mach and Reynolds Number Effects on the Characteristics of the Wing and on the Effectiveness of an Elevon. NACA RM A8D20, 1948.

3. McCormack, Gerald M., and Walling, Walter C.: Aerodynamic Study of a Wing-Fuselage Combination Employing a Wing Swept Back 63°.- Investigation of a Large-Scale Model at Low Speed. NACA RM A8D02, 1949.

4. Madden, Robert T.: Aerodynamic Study of a Wing-Fuselage Combination Employing a Wing Swept Back 63°.- Characteristics at a Mach Number of 1.53 Including Effect of Small Variations of Sweep. NACA RM A8J04, 1949.

5. Madden, Robert T.: Aerodynamic Study of a Wing-Fuselage Combination Employing a Wing Swept Back 63°.- Investigation at a Mach Number of 1.53 to Determine the Effects of Cambering and Twisting the Wing for Uniform Load at a Lift Coefficient of 0.25. NACA RM A9C07, 1949.

6. Jones, J. Lloyd, and Demele, Fred A.: Aerodynamic Study of a Wing-Fuselage Combination Employing a Wing Swept Back 63°.- Characteristics Throughout the Subsonic Speed Range with the Wing Cambered and Twisted for a Uniform Load at a Lift Coefficient of 0.25. NACA RM A9D25, 1949.

7. Jones, Robert T.: Estimated Lift-Drag Ratios at Supersonic Speed. NACA TN 1350, 1947.

8. Glauert, H.: Wind Tunnel Interference on Wings, Bodies and Aircrews. R. & M. No. 1566, British A. R. C., 1933.

9. Herriot, John G.: Blockage Corrections for Three-Dimensional-Flow Closed-Throat Wind Tunnels with Consideration of the Effect of Compressibility. NACA RM A7B28, 1947.

10. Swanson, Robert S., and Priddy, E. LaVerne: Lifting-Surface-Theory Values of the Damping in Roll and of the Parameter Used in Estimating Aileron Stick Forces. NACA ARR L5F23, 1945.

11. Polhamus, Edward C.: A Simple Method of Estimating the Subsonic Lift and Damping in Roll of Sweptback Wings. NACA TN 1862, 1949.

TABLE I.- AIRFOIL-SECTION COORDINATES

[All values given in percent chord]

c_0

Lower surface		Upper surface	
Station	Ordinate	Station	Ordinate
0	0	0	0
.5	-.404	.5	.404
.75	-.488	.75	.488
1.25	-.616	1.25	.616
2.50	-.847	2.50	.847
5.00	-1.166	5.00	1.166
10.0	-1.599	10.0	1.599
20.0	-2.131	20.0	2.131
30.0	-2.413	30.0	2.413
40.0	-2.499	40.0	2.499
50.0	-2.354	50.0	2.354
60.0	-2.032	60.0	2.032
70.0	-1.589	70.0	1.589
80.0	-1.071	80.0	1.071
90.0	-.541	90.0	.541
100.0	-.011	100.0	.011

c_1

Lower surface		Upper surface	
Station	Ordinate	Station	Ordinate
0	0	0	0
.526	-.366	.474	.438
.778	-.433	.726	.536
1.283	-.536	1.221	.690
2.535	-.706	2.463	.984
5.039	-.927	4.956	1.401
10.041	-1.211	9.959	1.984
20.036	-1.530	19.964	2.725
30.026	-1.685	29.974	3.138
40.010	-1.700	39.990	3.297
50.00	-1.530	50.000	3.179
59.990	-1.231	60.010	2.828
69.985	-.860	70.015	2.313
79.985	-.479	80.015	1.669
89.985	-.155	90.015	.927
100.000	- - -	100.000	- - -

c_2

Lower surface		Upper surface	
Station	Ordinate	Station	Ordinate
0	0	0	0
.532	-.357	.469	.457
.788	-.419	.713	.557
1.295	-.507	1.208	.720
2.547	-.663	2.447	1.026
5.056	-.851	4.944	1.477
10.056	-1.089	9.944	2.103
20.044	-1.345	19.956	2.912
30.031	-1.458	29.969	3.373
40.013	-1.446	39.987	3.548
50.000	-1.270	50.000	3.436
59.987	-.982	60.013	3.085
69.981	-.632	70.019	2.547
79.975	-.288	80.025	1.852
89.981	-.031	90.019	1.045
100.000	- - -	100.000	- - -

c_3

Lower surface		Upper surface	
Station	Ordinate	Station	Ordinate
0.533	-0.350	0.470	0.462
.788	-.414	.709	.557
1.298	-.502	1.202	.725
2.556	-.645	2.444	1.043
5.056	-.828	4.944	1.497
10.056	-1.051	9.944	2.150
20.048	-1.290	19.952	2.978
30.032	-1.377	29.968	3.447
40.016	-1.361	39.984	3.639
50.000	-1.186	50.000	3.527
59.984	-.892	60.016	3.169
69.976	-.557	70.024	2.627
79.976	-.223	80.024	1.911
89.984	.008	90.016	1.091
100.000	- - -	100.000	- - -

c_4

Lower surface		Upper surface	
Station	Ordinate	Station	Ordinate
0.536	-0.350	0.470	0.460
.799	-.405	.711	.558
1.291	-.503	1.204	.722
2.549	-.646	2.440	1.039
5.055	-.832	4.945	1.489
10.055	-1.050	9.945	2.144
20.044	-1.291	19.956	2.976
30.033	-1.389	29.967	3.425
40.022	-1.368	39.978	3.621
50.000	-1.193	50.000	3.512
59.989	-.908	60.011	3.162
69.978	-.569	70.022	2.604
79.978	-.230	80.022	1.915
89.978	.011	90.022	1.083
100.000	- - -	100.000	- - -

c_5

Lower surface		Upper surface	
Station	Ordinate	Station	Ordinate
0.543	-0.350	0.473	0.455
.788	-.420	.718	.560
1.278	-.508	1.208	.718
2.557	-.648	2.452	1.033
5.061	-.823	4.956	1.494
10.070	-1.068	9.965	2.119
20.053	-1.313	19.947	2.960
30.035	-1.419	29.965	3.415
40.018	-1.401	39.982	2.608
50.000	-1.208	50.000	3.485
59.982	-.928	60.018	3.135
69.982	-.595	70.018	2.592
79.982	-.245	80.018	1.891
89.982	-.018	90.018	1.068
100.000	- - -	100.000	- - -

Note: Spanwise positions of airfoil sections c_0 to c_5 are shown in figure 3.
For all sections: Leading-edge radius = 0.175. Trailing-edge radius = 0.014.

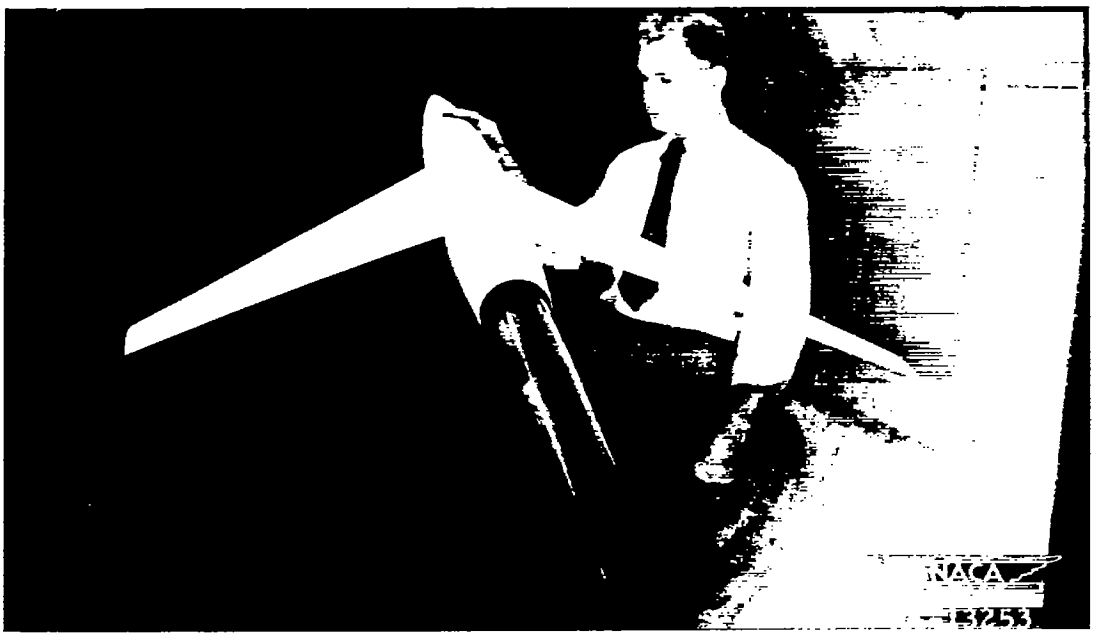

(a) Rear view.

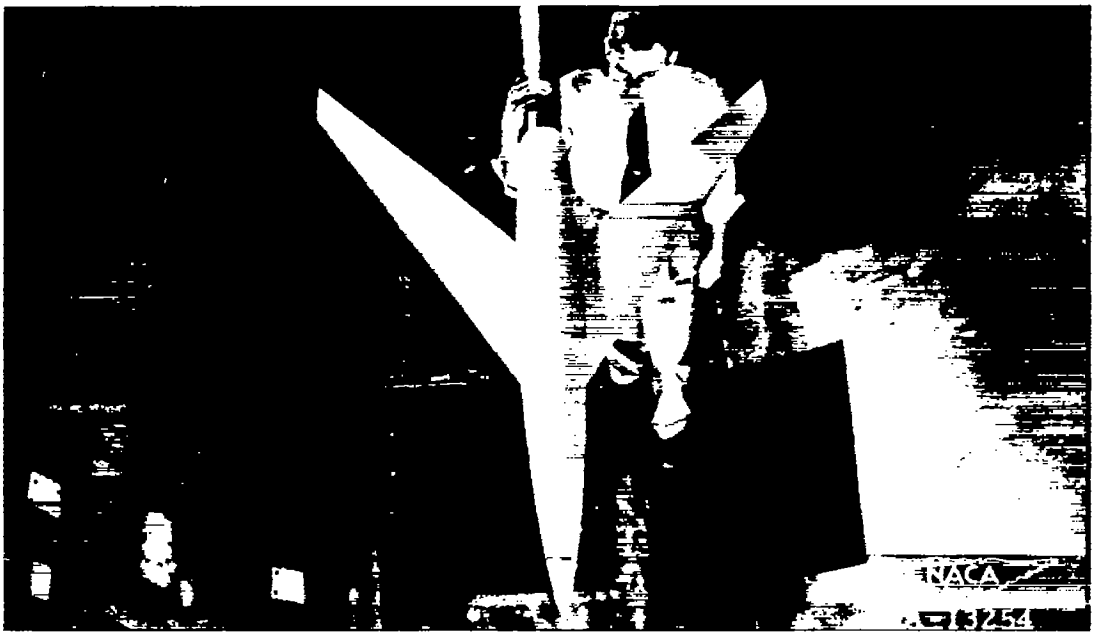

(b) Plan view.

Figure 1.— Model of the cambered and twisted wing with the leading edge swept back 63° in combination with a fuselage.

Equation for fuselage ordinates:

$$\frac{r}{r_{max}} = \left[1 - \left(1 - \frac{2x}{l}\right)^2\right]^{\frac{3}{4}}$$

Note: All dimensions given in feet unless otherwise specified.

Fineness ratio; $\frac{l}{2r_{max}} = 12.5$

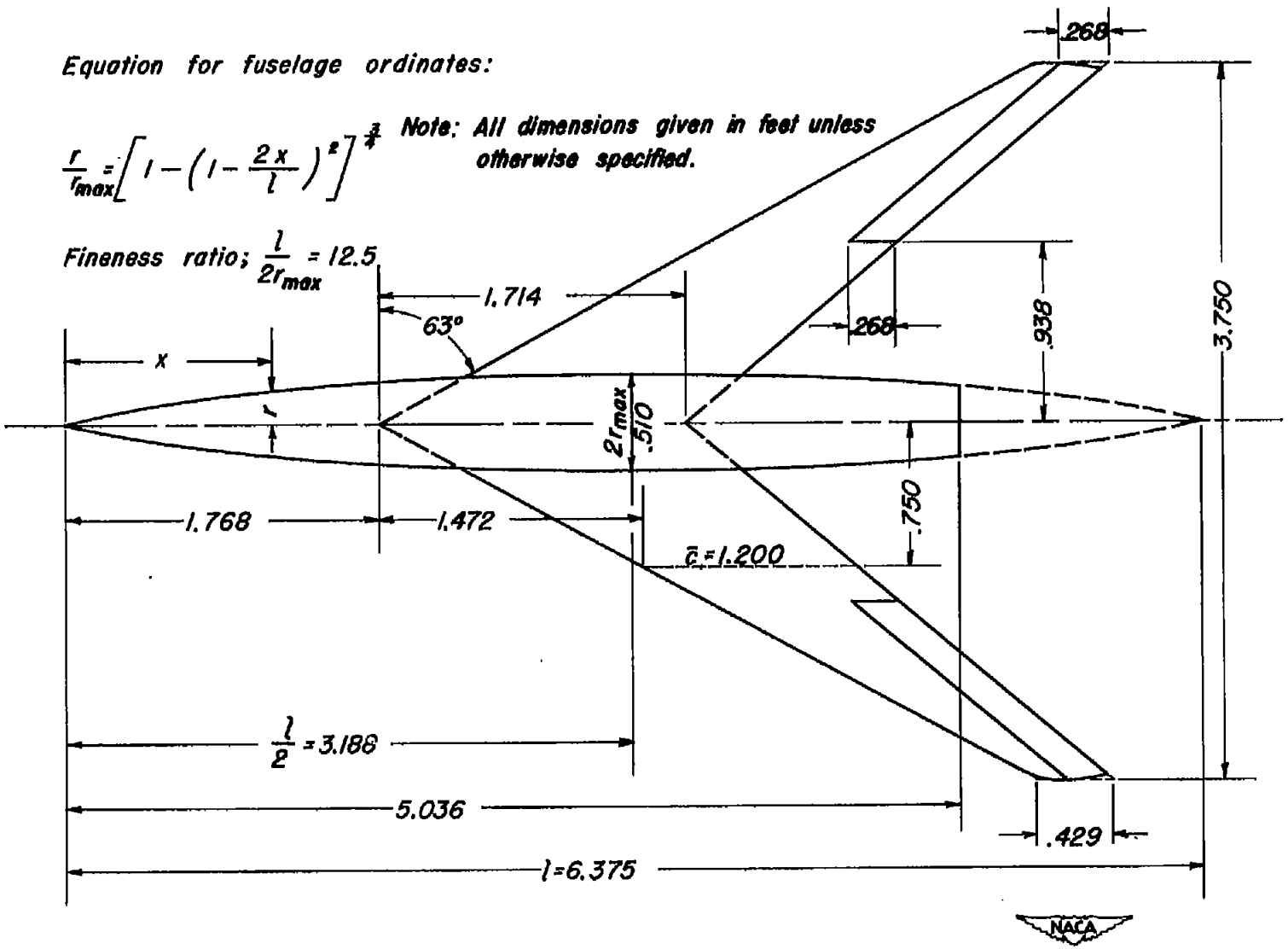

Figure 2.— Dimensions of wing and fuselage.

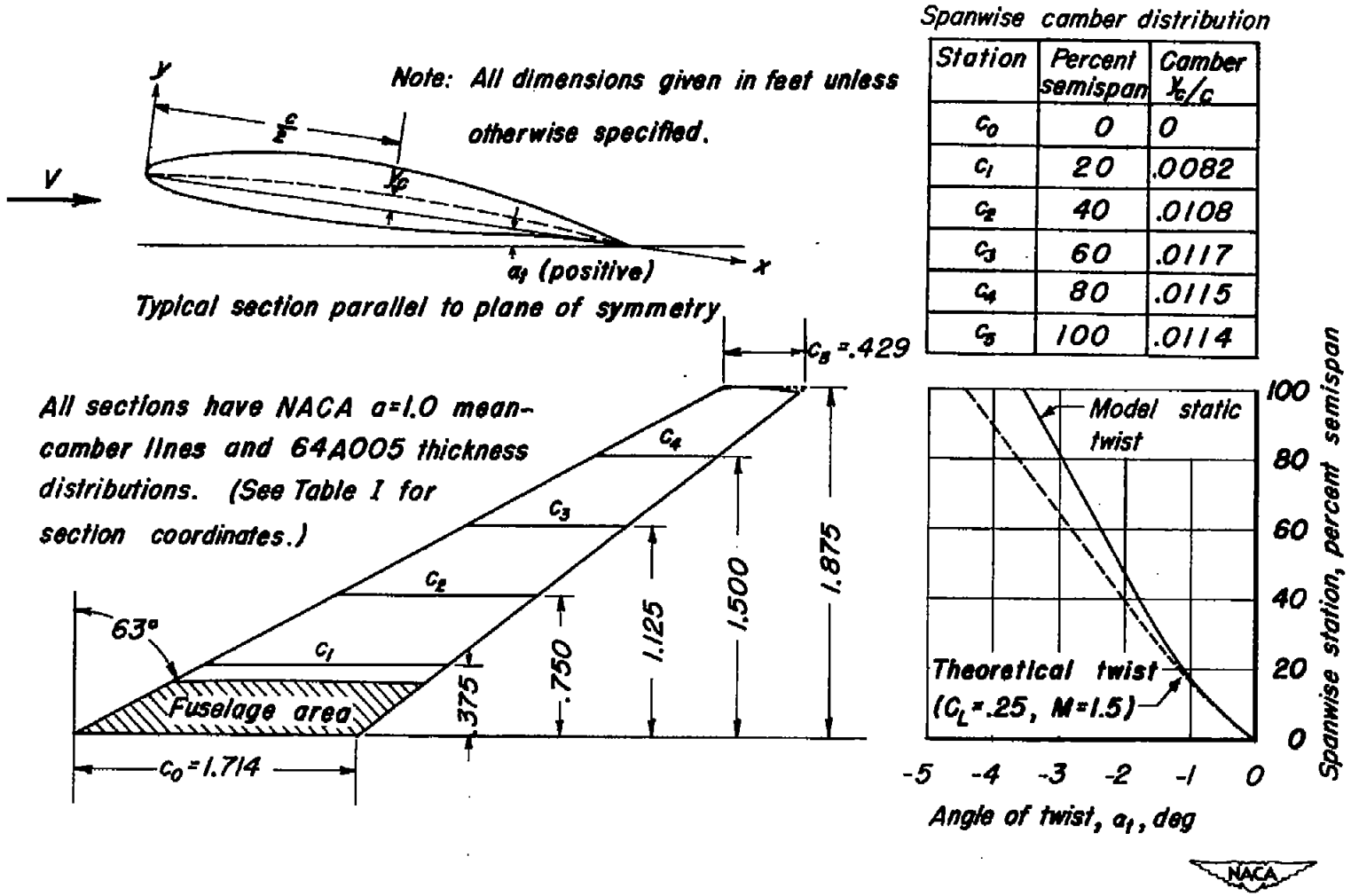

Station	Percent semispan	Camber y_c/c
c_0	0	0
c_1	20	.0082
c_2	40	.0108
c_3	60	.0117
c_4	80	.0115
c_5	100	.0114

Figure 3.— Plan form of right half of wing showing spanwise variation of camber and twist and location of sections for which coordinates have been calculated.

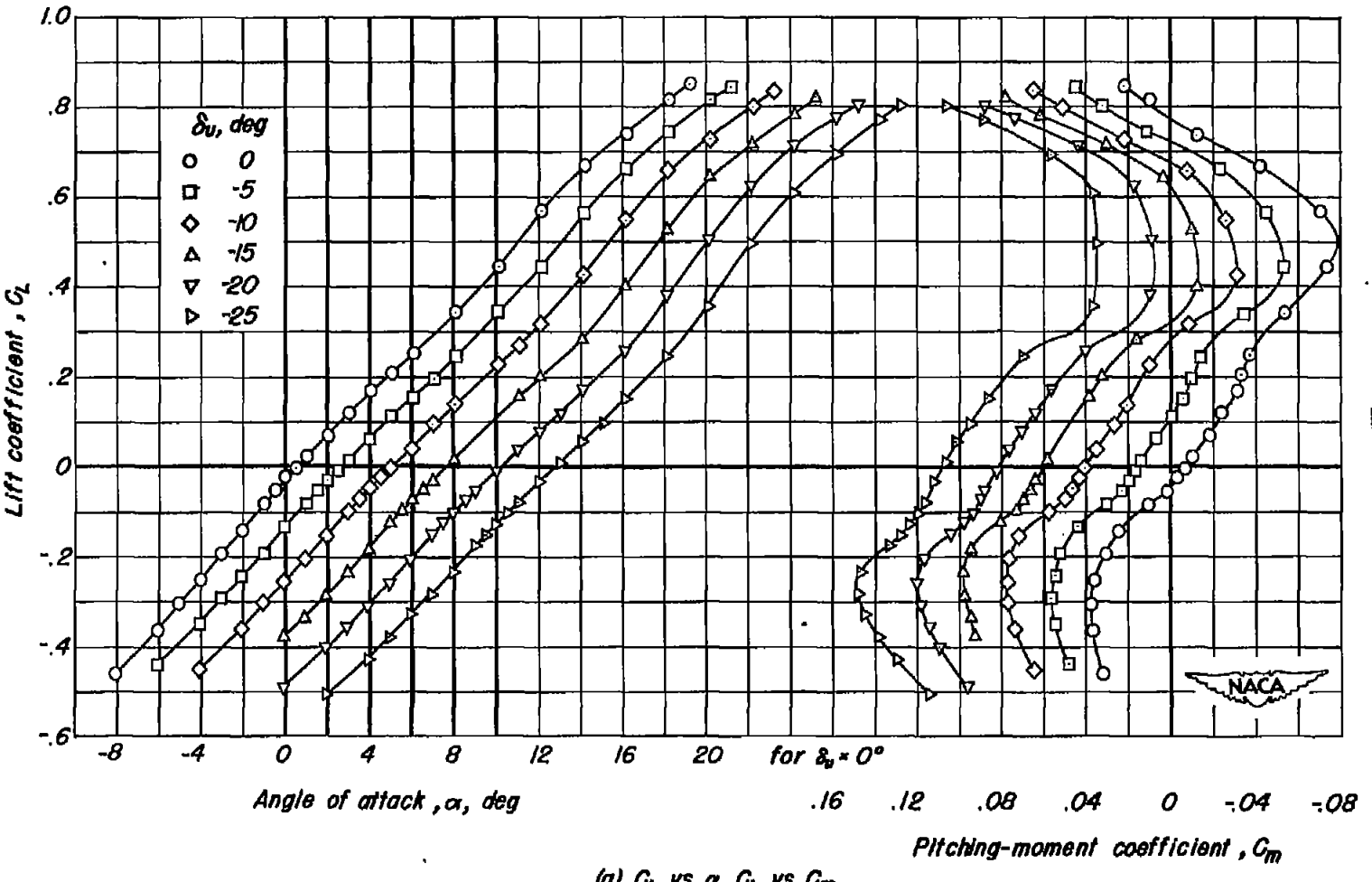

(a) C_L vs α, C_L vs C_m.

Figure 4.- The effect of elevon deflection on the aerodynamic characteristics of the wing-fuselage combination and on the elevon hinge-moment coefficients at a Mach number of 0.20.

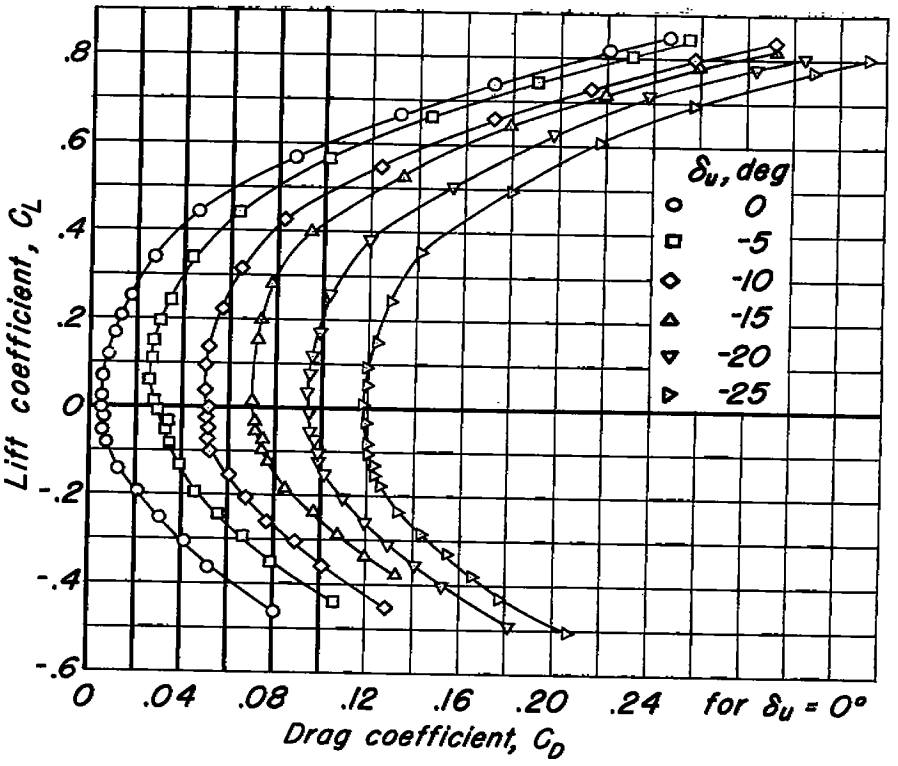

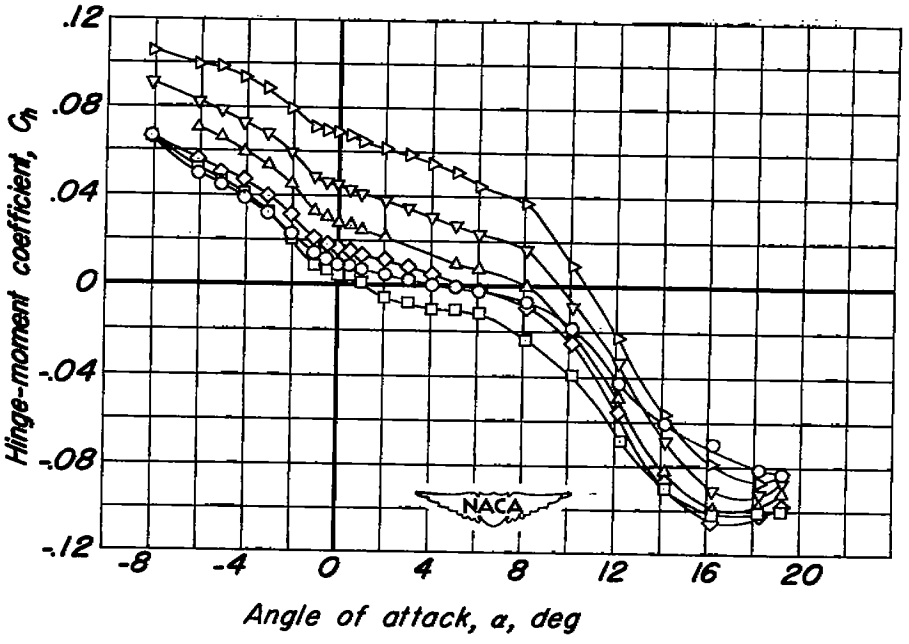

(b) C_L vs C_D, C_h vs α.

Figure 4.- Concluded.

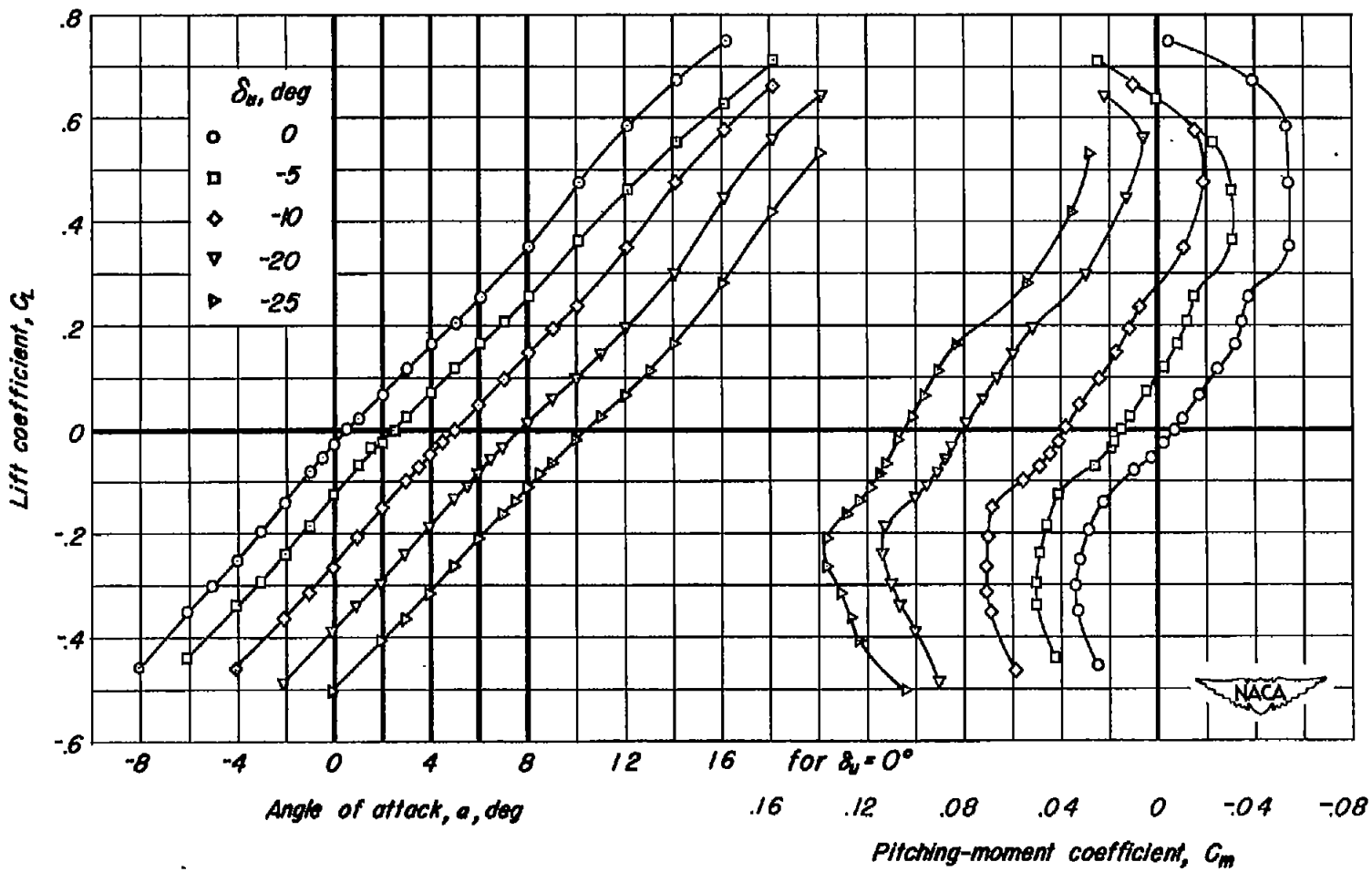

(a) C_L vs α, C_L vs C_m.

Figure 5.- The effect of elevon deflection on the aerodynamic characteristics of the wing-fuselage combination and on the elevon hinge-moment coefficients at a Mach number of 0.60.

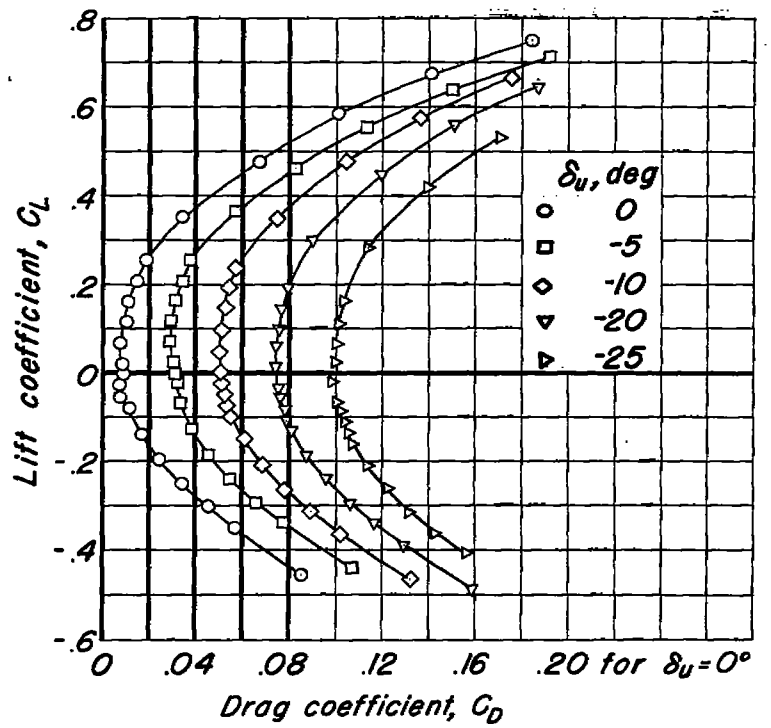

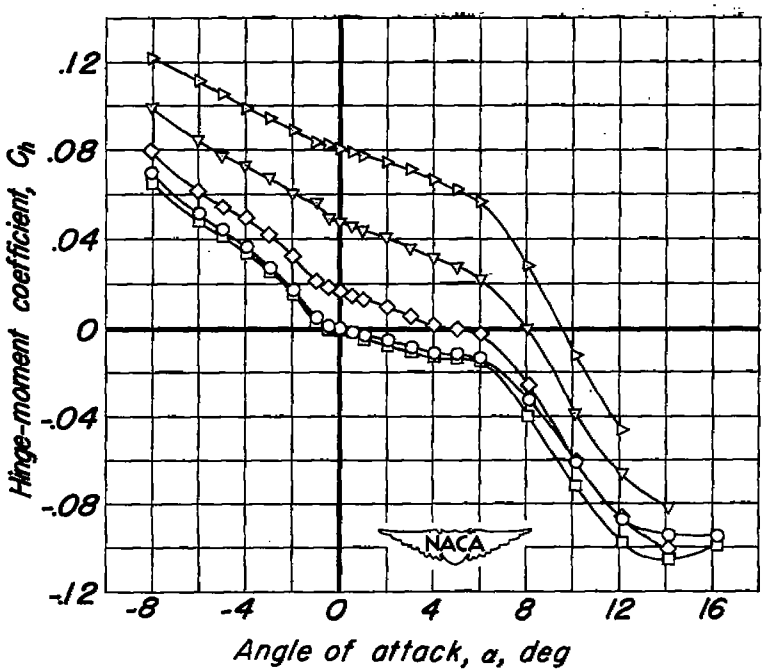

(b) C_L vs C_D, C_h vs α.

Figure 5.- Concluded.

[redacted]

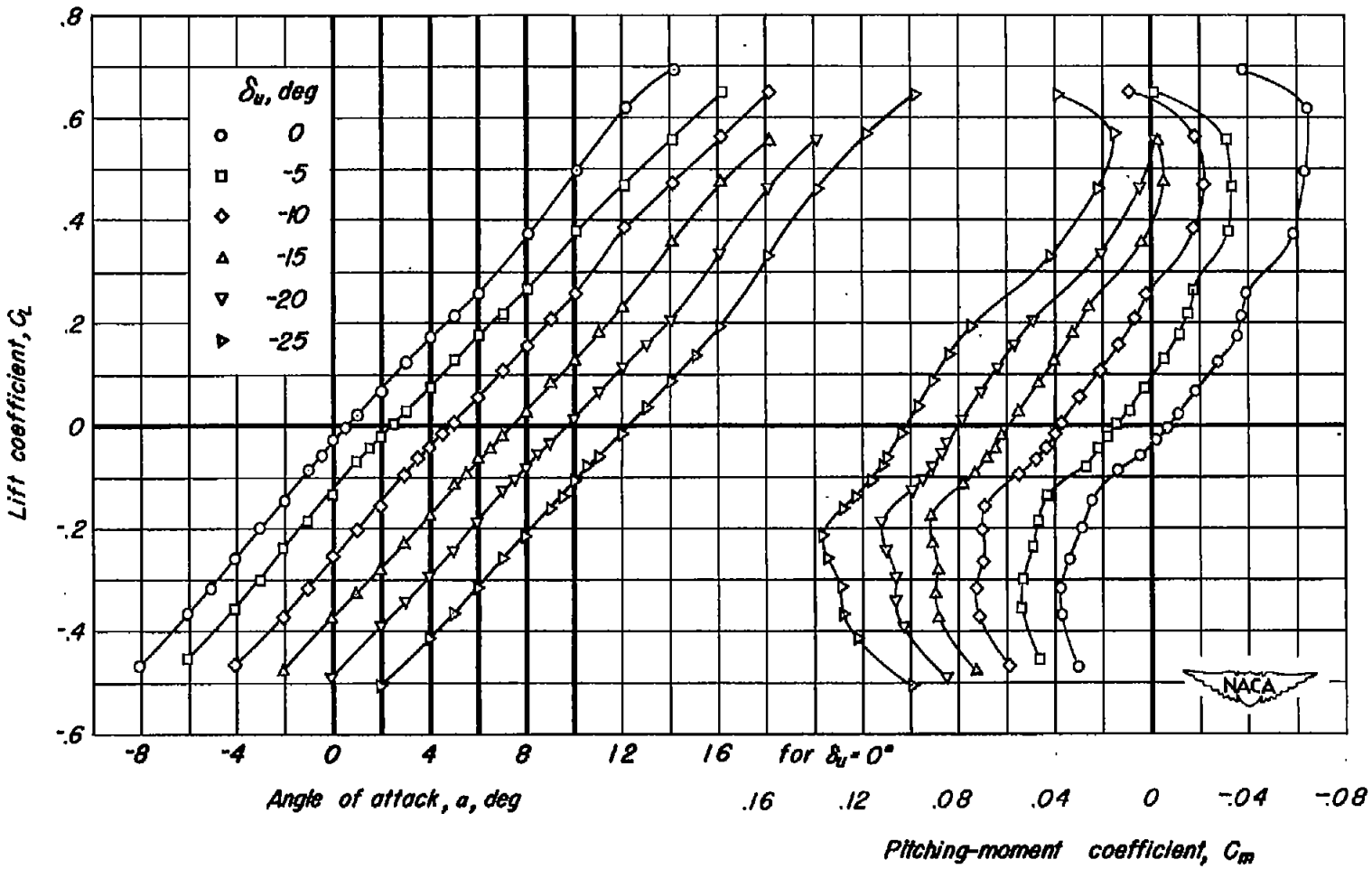

(a) C_L vs α, C_L vs C_m.

Figure 6.- The effect of elevon deflection on the aerodynamic characteristics of the wing-fuselage combination and on the elevon hinge-moment coefficients at a Mach number of 0.80.

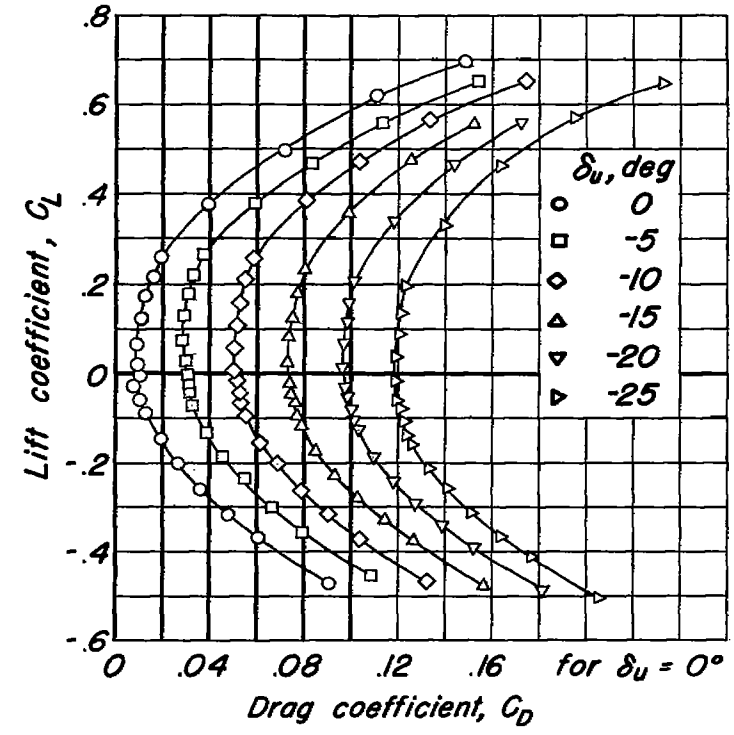

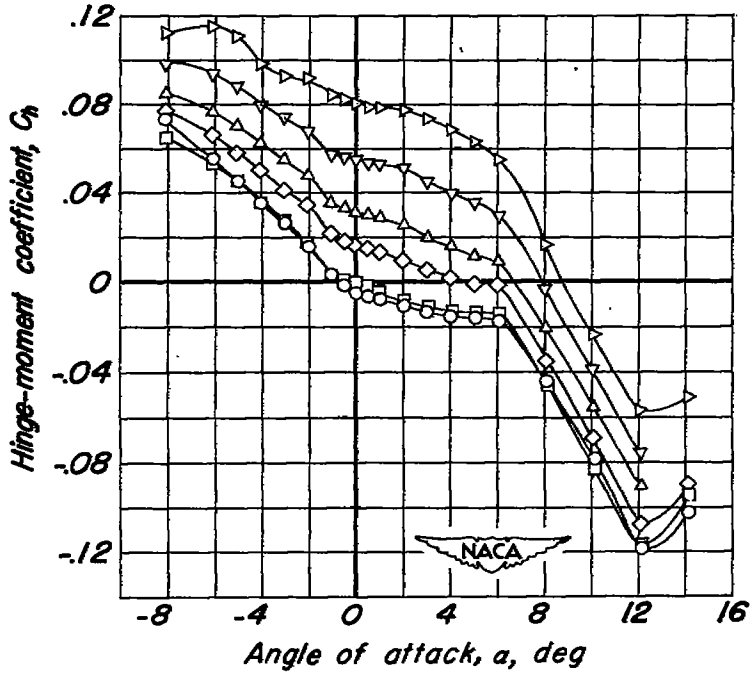

(b) C_L vs C_D, C_h vs α.

Figure 6.- Concluded.

[redacted]

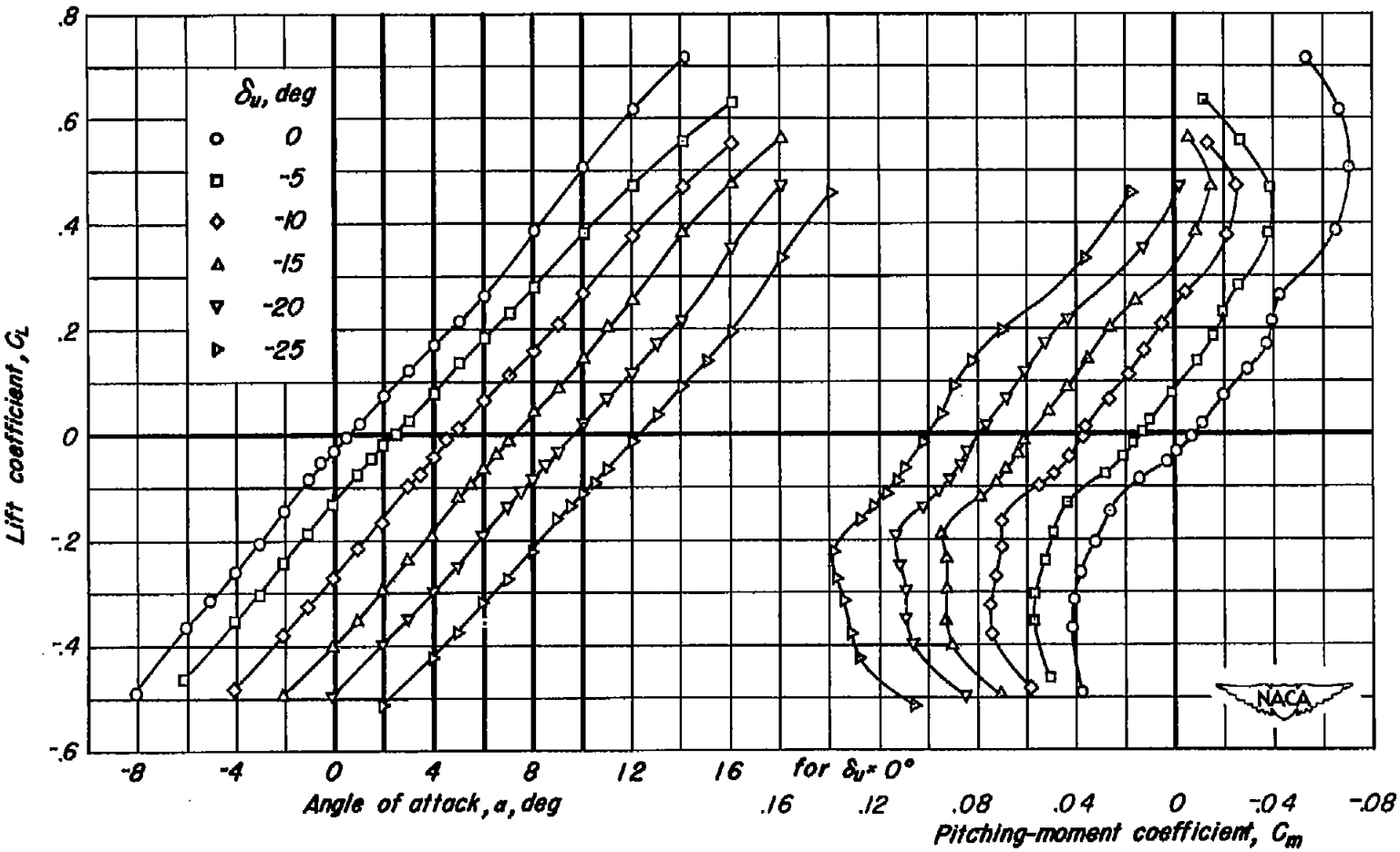

(a) C_L vs α, C_L vs C_m.

Figure 7.- The effect of elevon deflection on the aerodynamic characteristics of the wing-fuselage combination and on the elevon hinge-moment coefficients at a Mach number of 0.89.

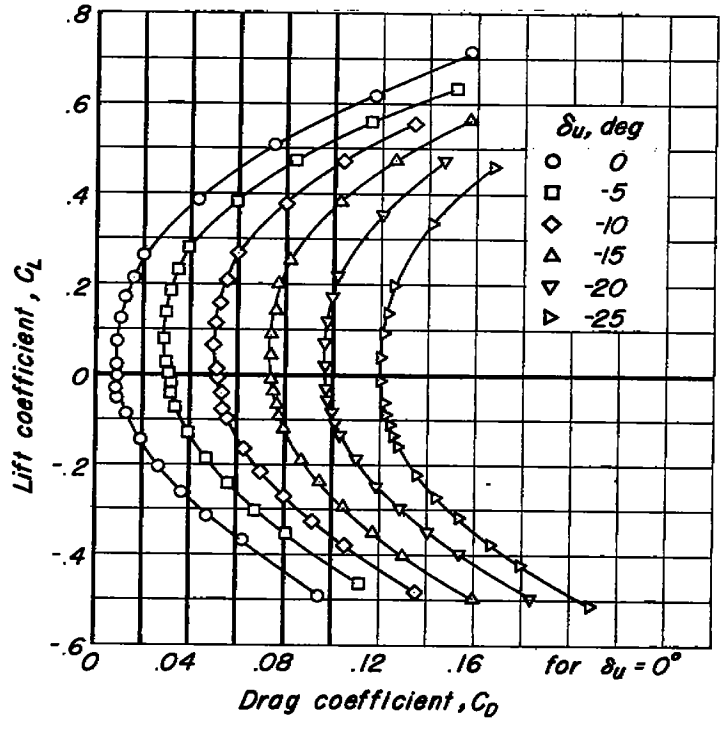

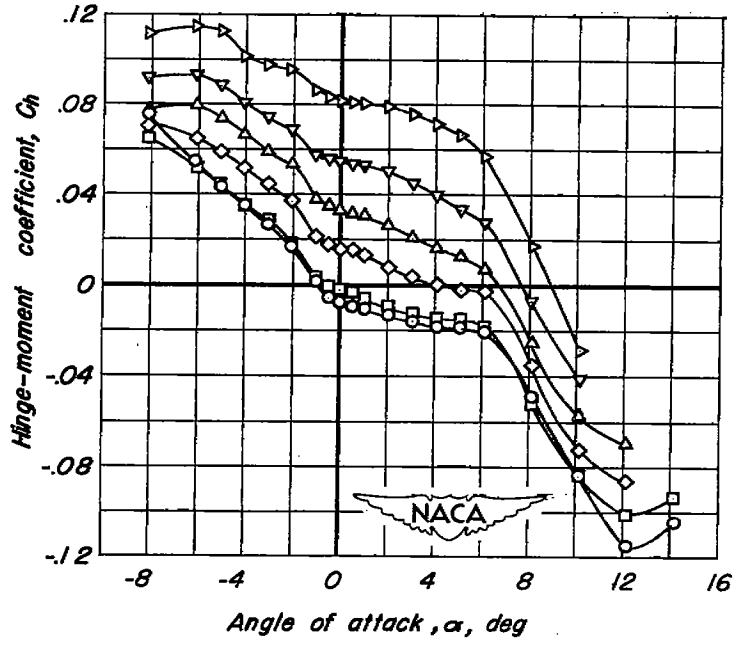

(b) C_L vs C_D, C_h vs α.

Figure 7.– Concluded.

[redacted]

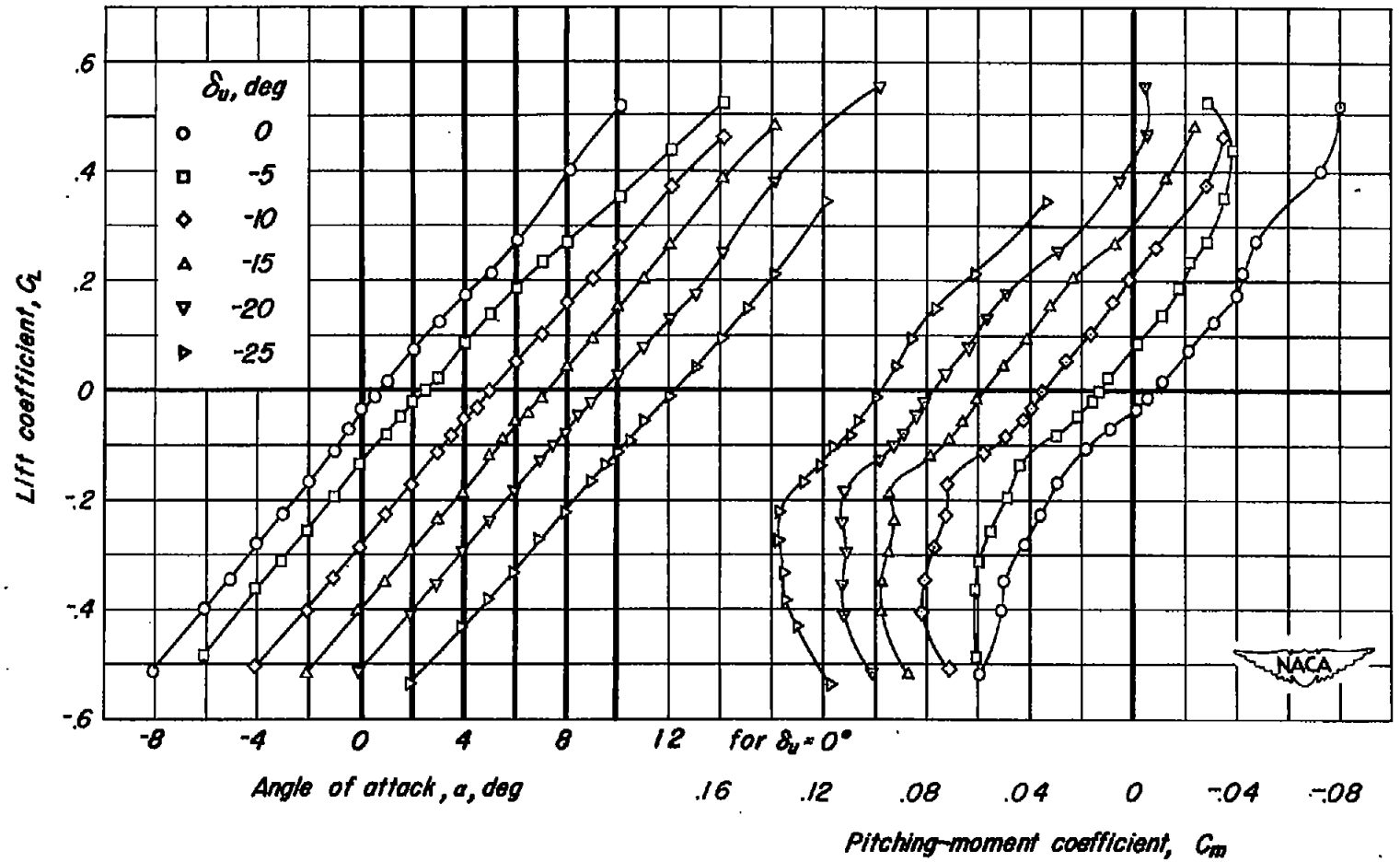

(a) C_L vs α, C_L vs C_m.

Figure 8.– The effect of elevon deflection on the aerodynamic characteristics of the wing-fuselage combination and on the elevon hinge-moment coefficients at a Mach number of 0.93.

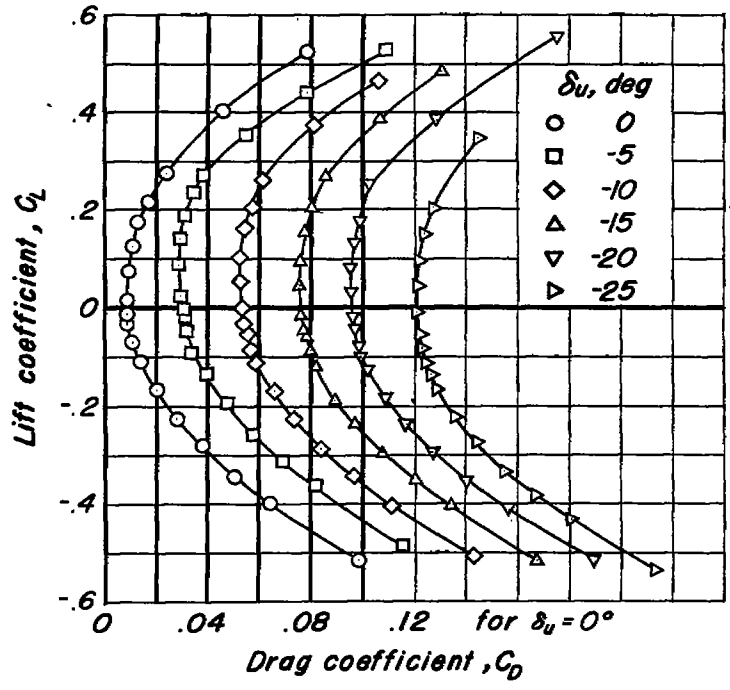

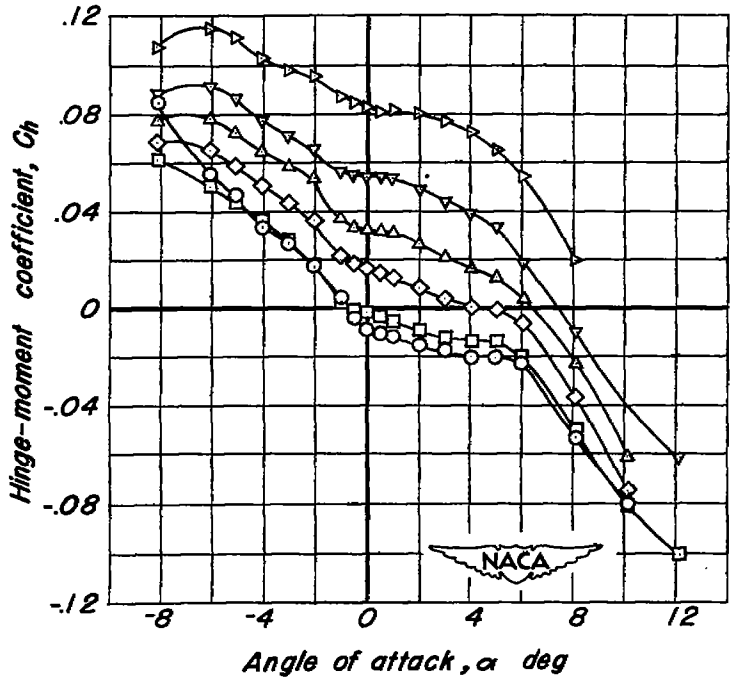

(b) C_L vs C_D, C_h vs α.

Figure 8.– Concluded.

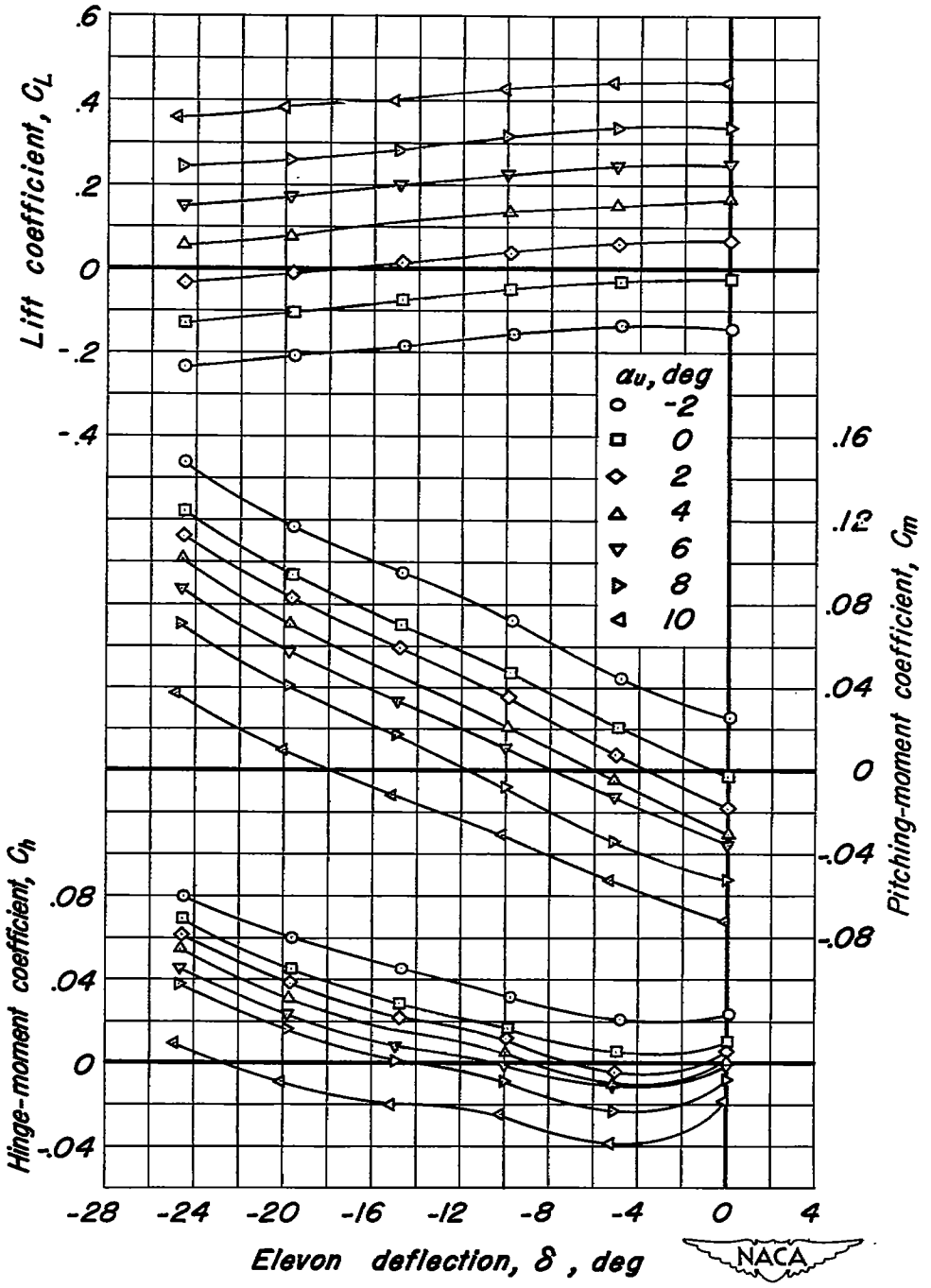

(a) M, 0.20.

Figure 9.– The variation of lift, pitching-moment, and hinge-moment coefficients with elevon deflection for various angles of attack at several Mach numbers.

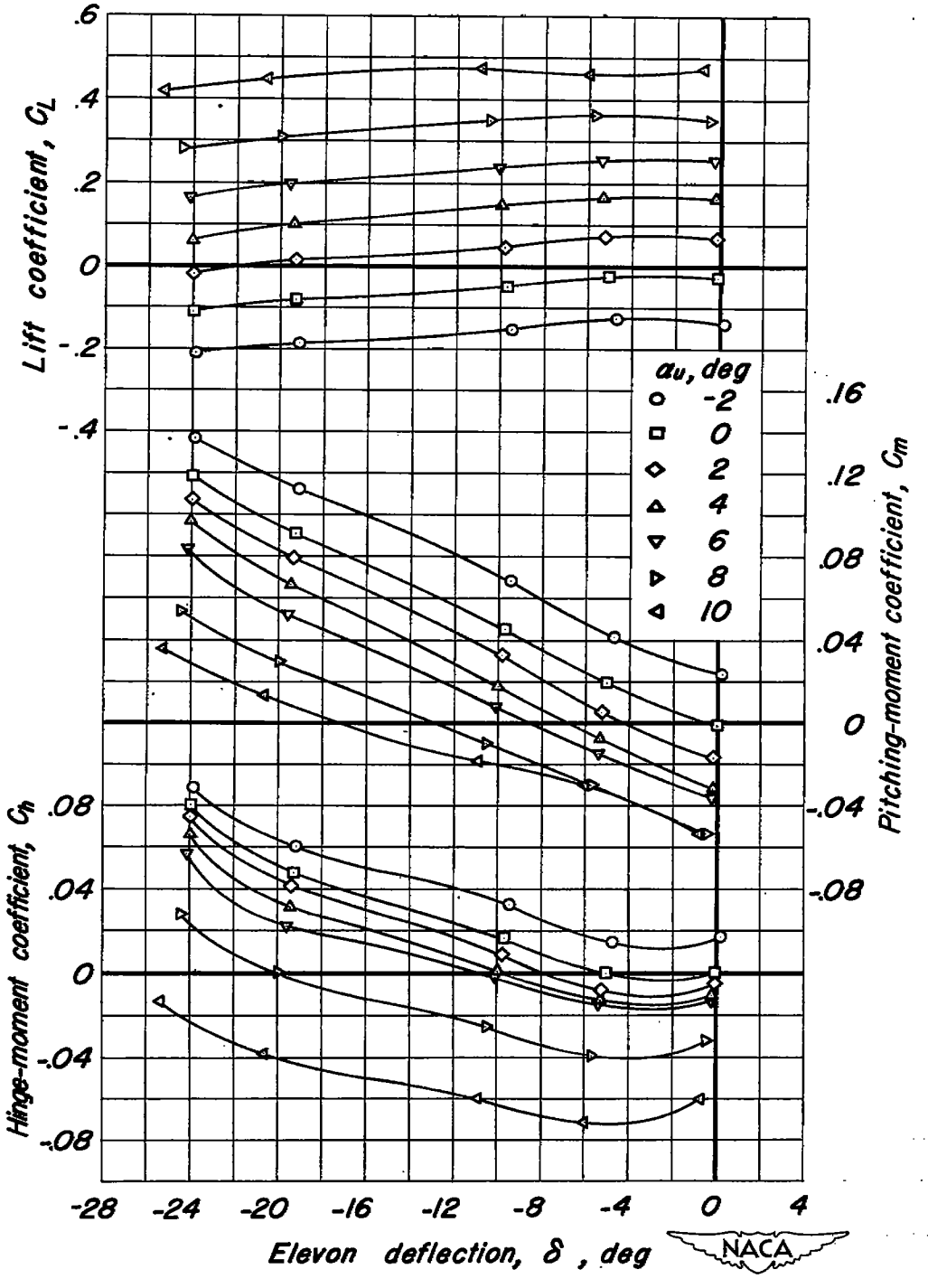

(b) M, 0.60.

Figure 9.- Continued.

[redacted]

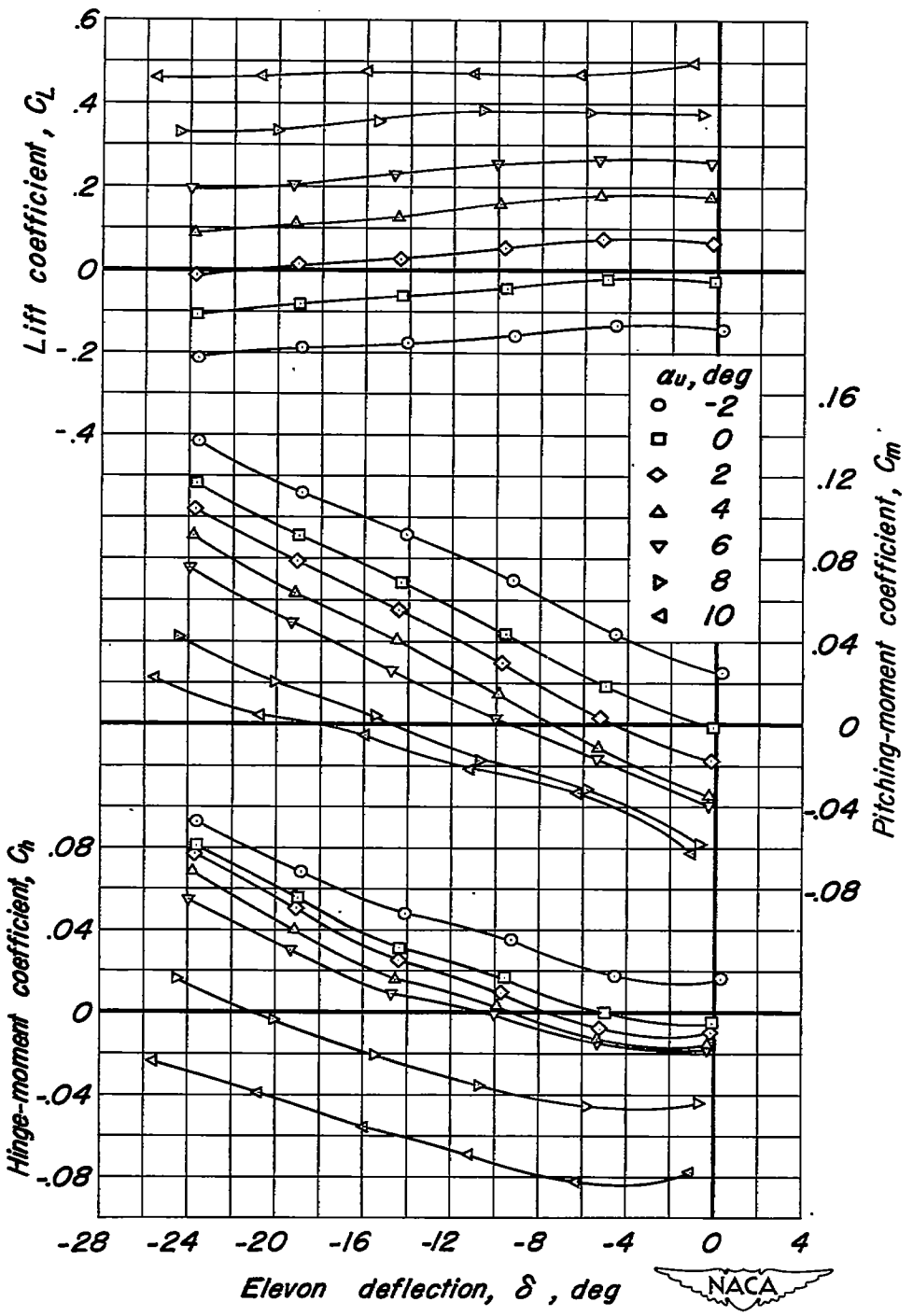

(c) M, 0.80.

Figure 9.- Continued.

[redacted]

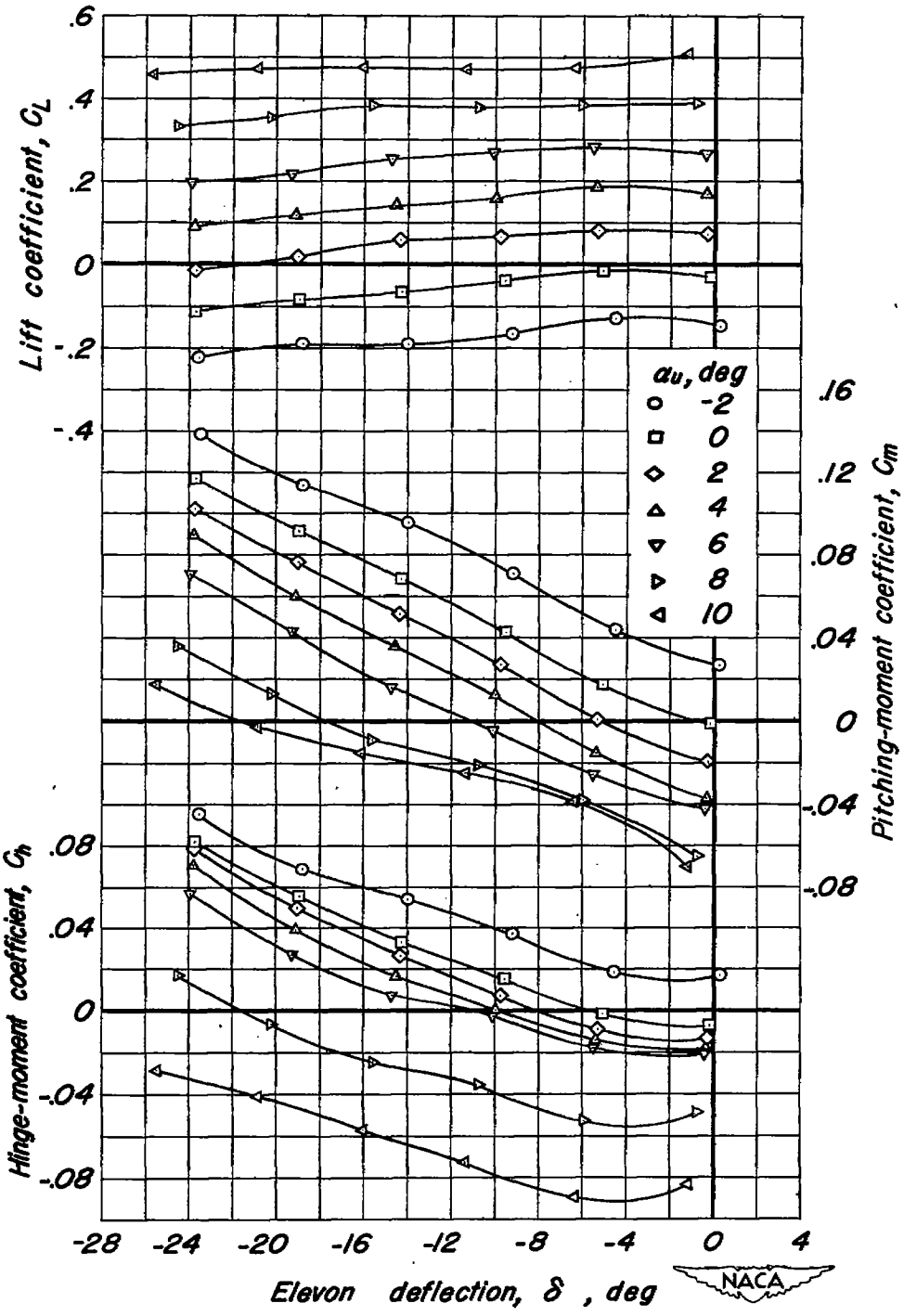

(d) M, 0.89.

Figure 9.- Continued.

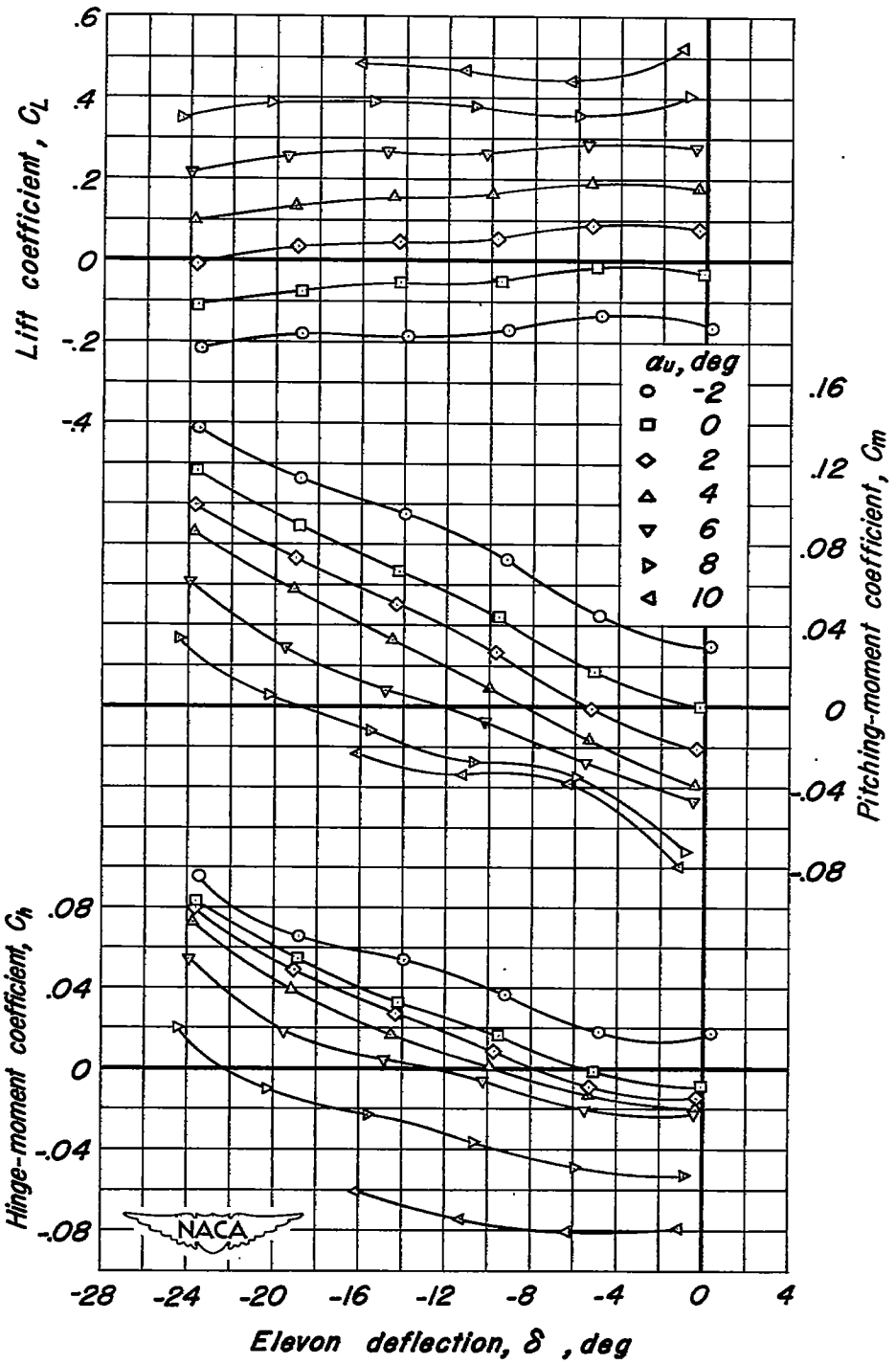

(e) M, 0.93.

Figure 9.– Concluded.

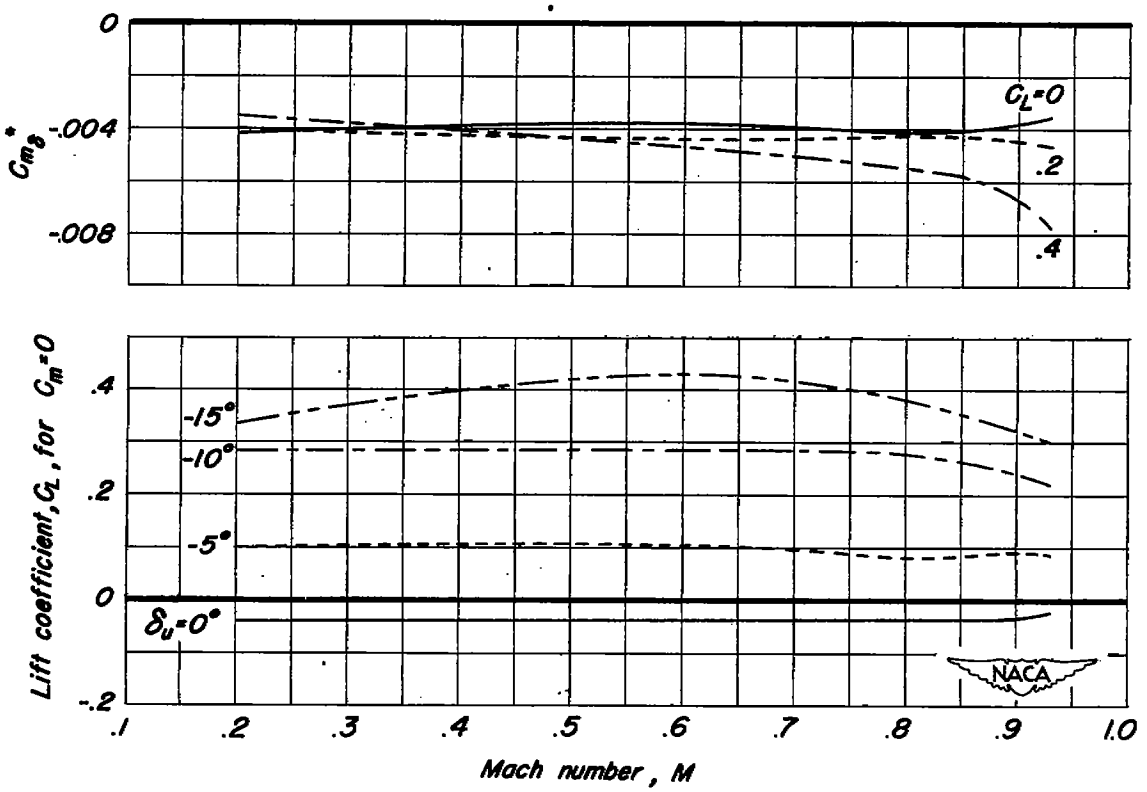

Figure 10.- The effect of Mach number on $C_{m_\delta}^*$ and on the lift coefficient for longitudinal balance.

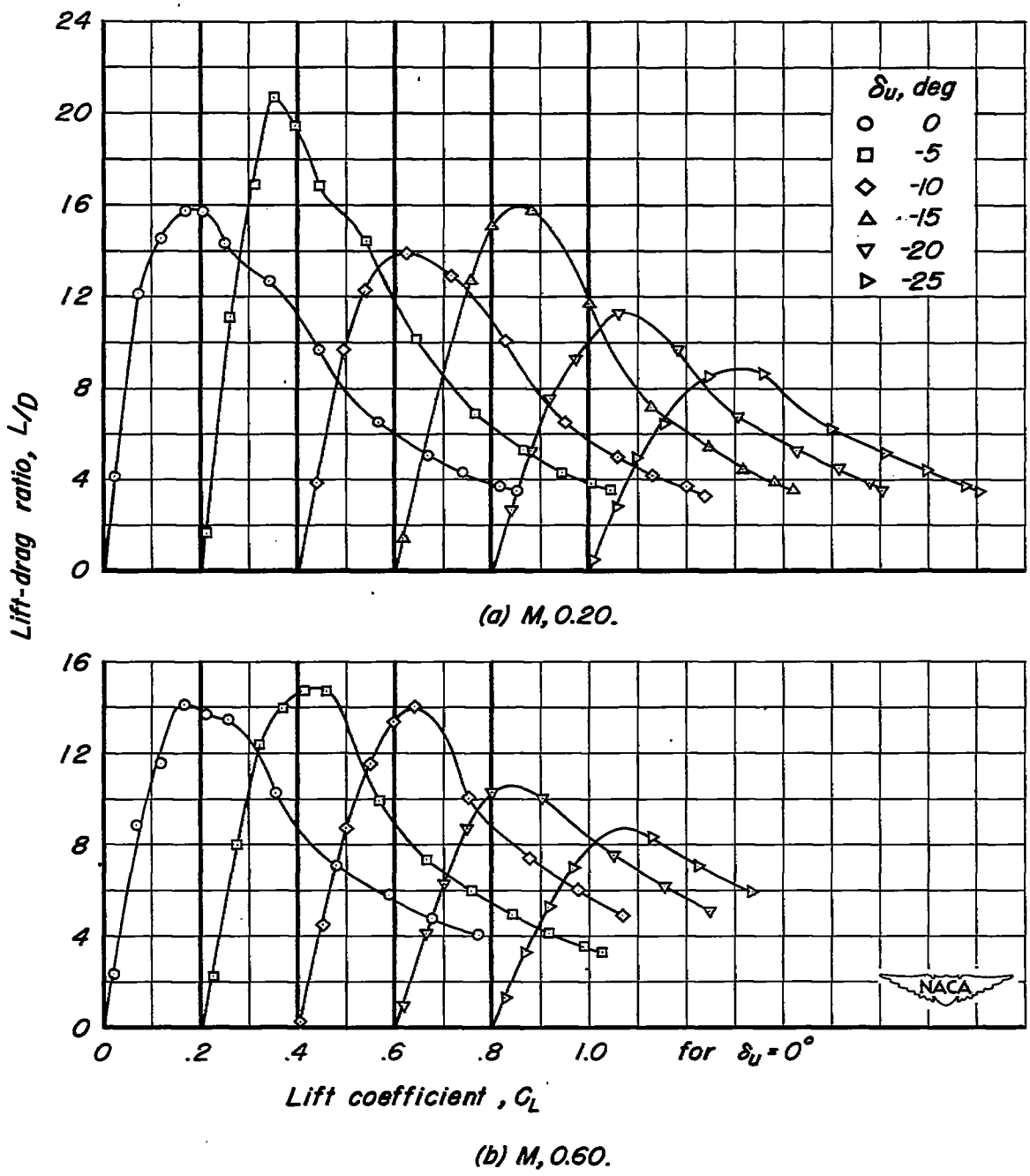

Figure 11.- The variation of lift-drag ratio with lift coefficient for various elevon deflections at several Mach numbers.

[redacted]

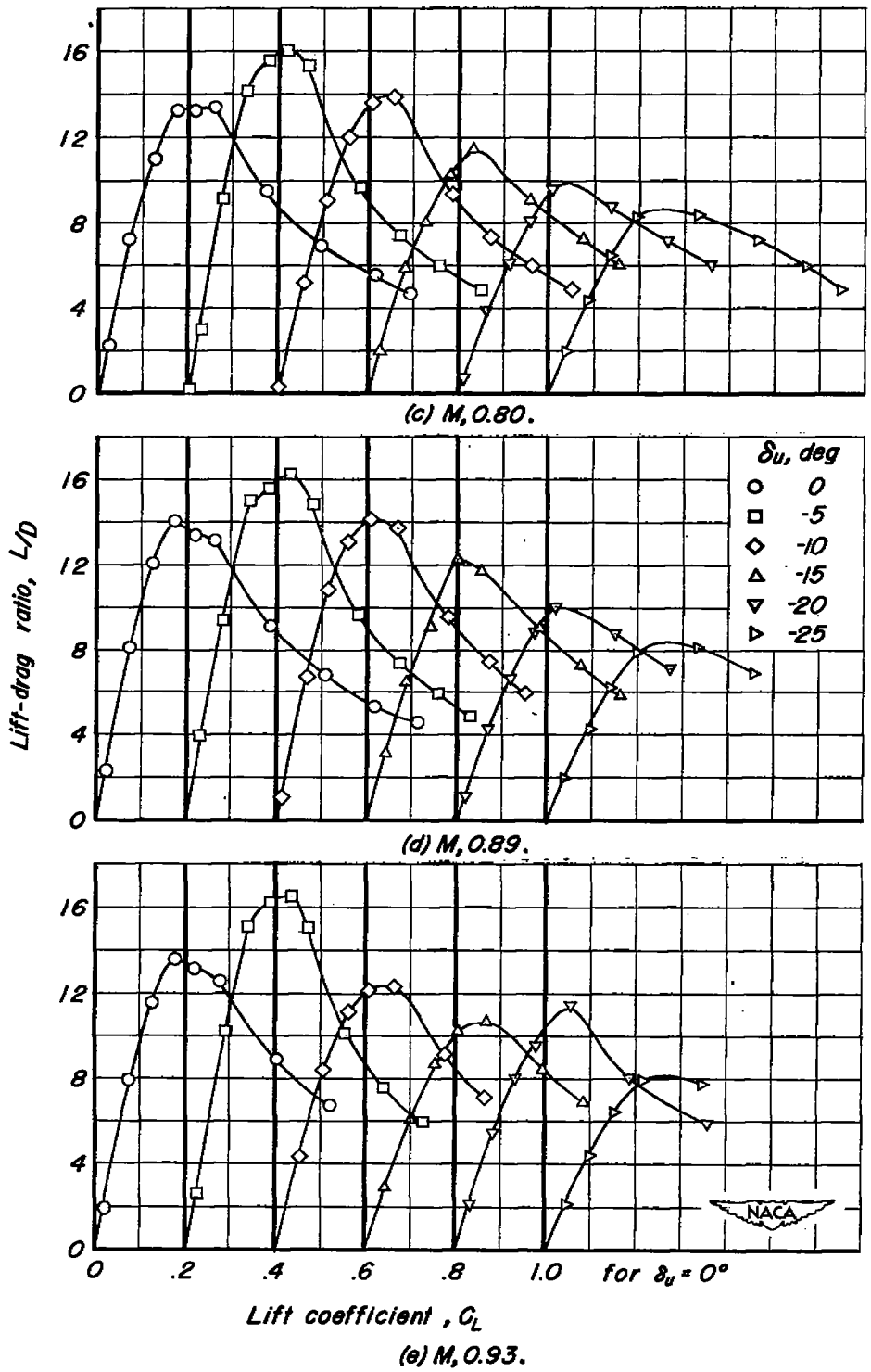

Figure 11.- Concluded.

[redacted]

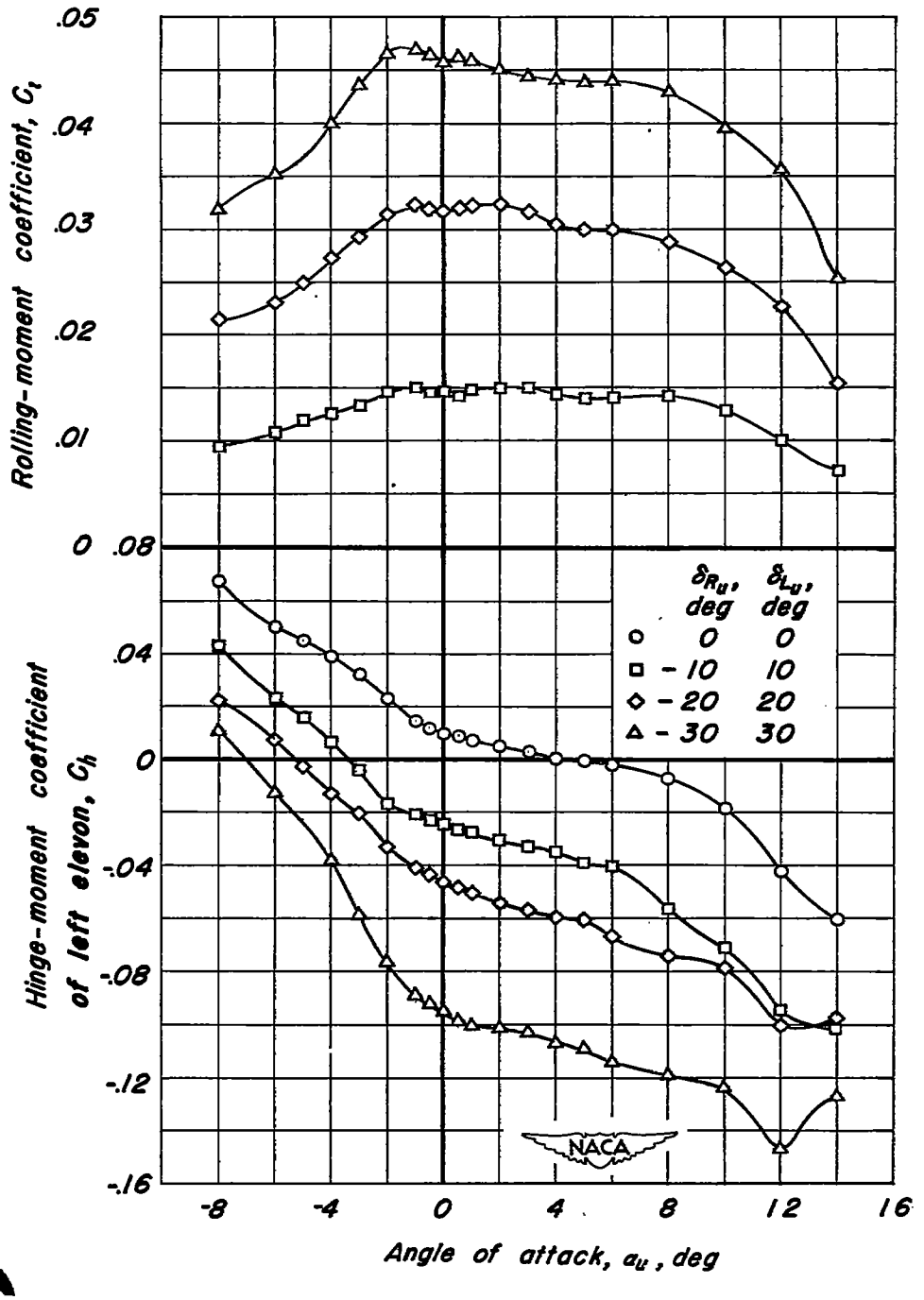

(a) M, 0.20.

Figure 12.- The variation of rolling-moment and hinge-moment coefficients with angle of attack for various elevon deflections at several Mach numbers.

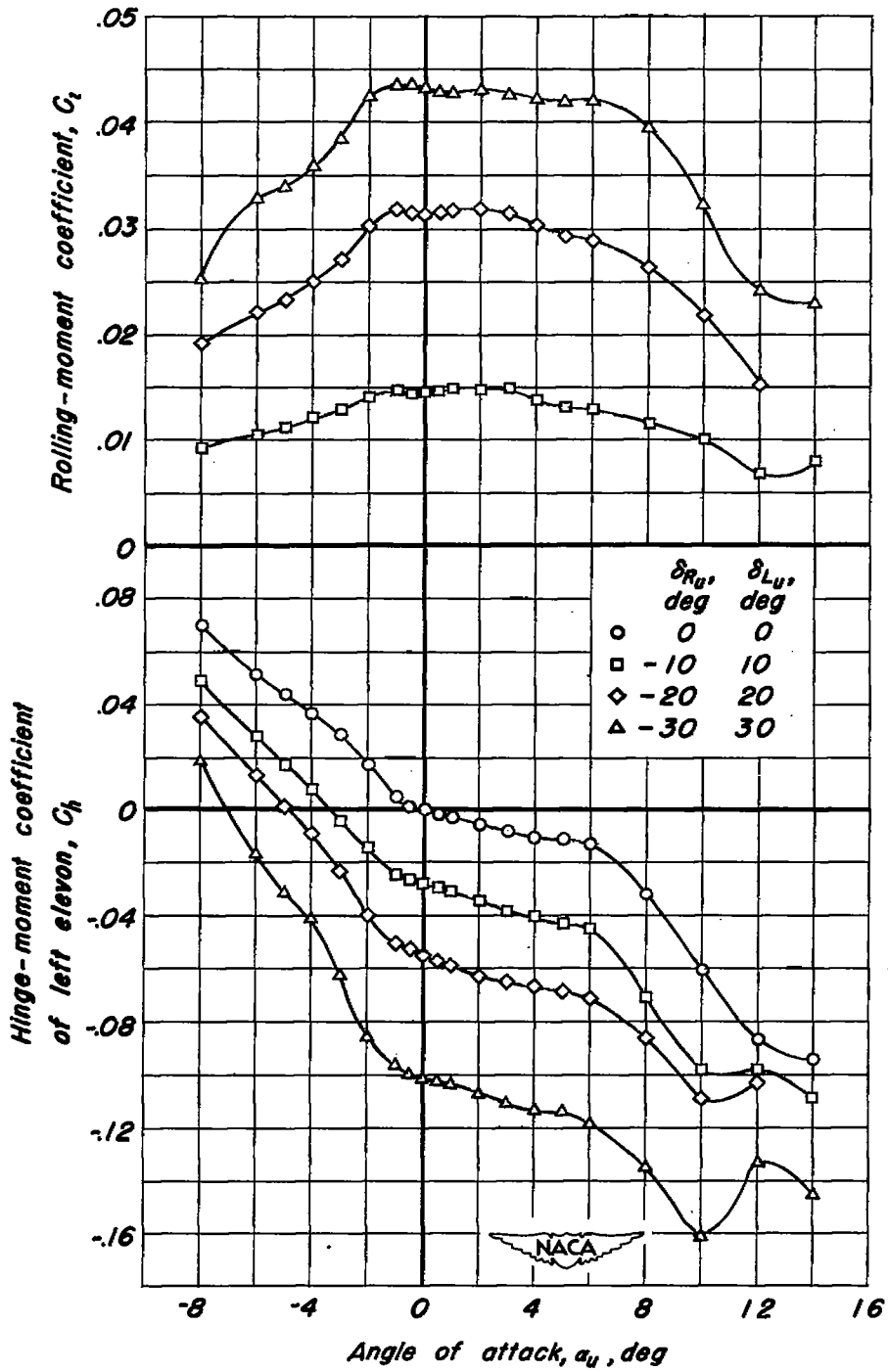

(b) M, 0.60.

Figure 12.- Continued.

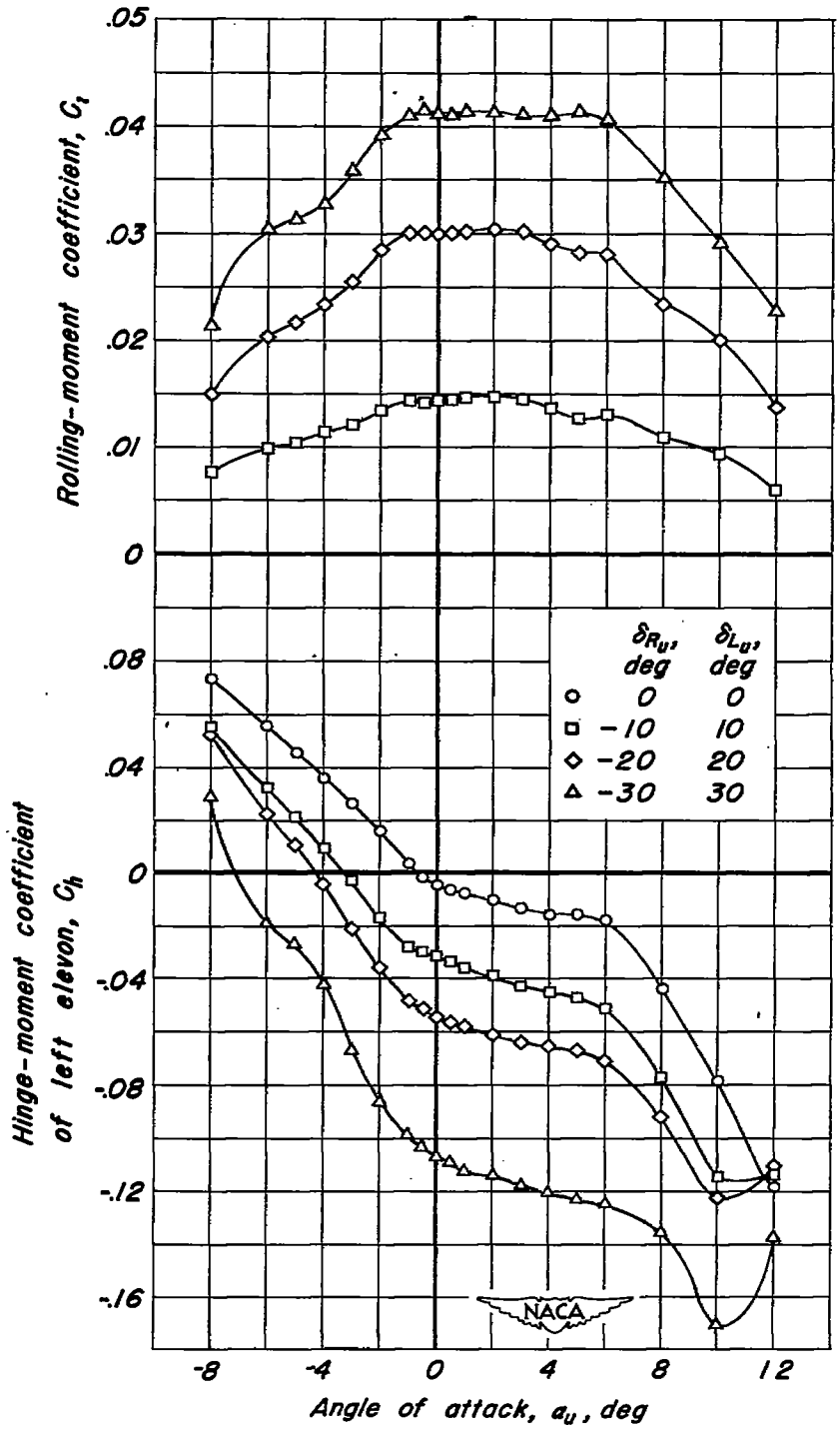

(c) M, 0.80.

Figure 12.- Continued.

[redacted]

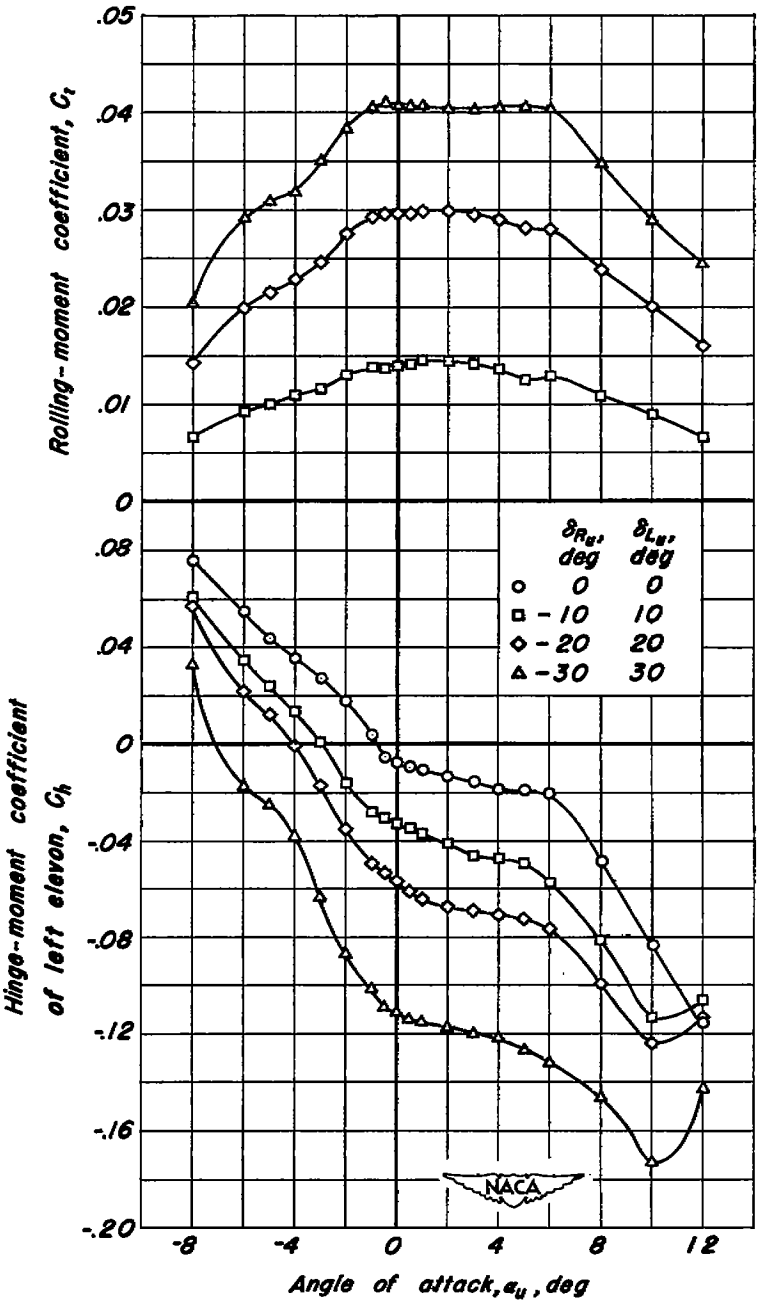

(d) M, 0.89.

Figure 12.- Continued.

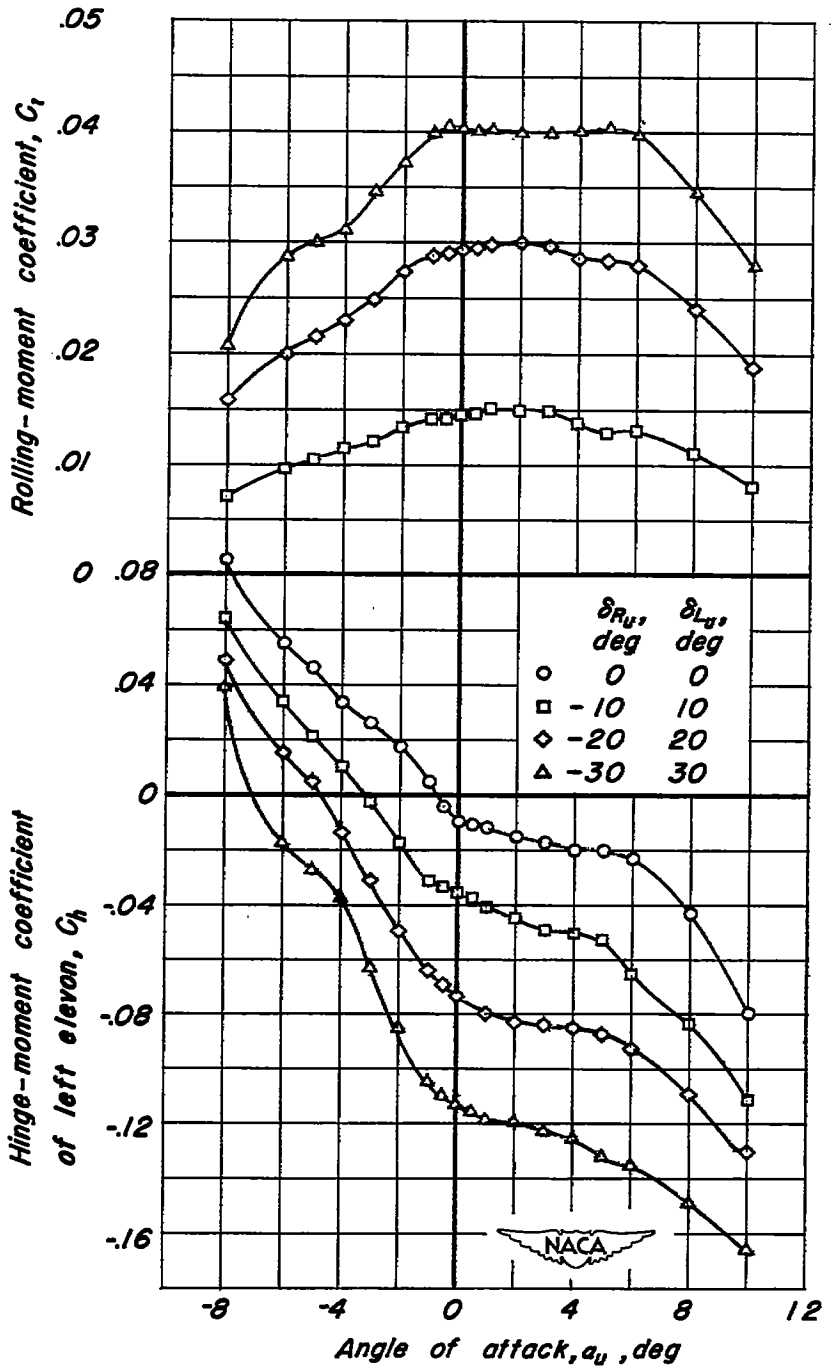

(e) M, 0.93.

Figure 12.- Concluded.

[redacted]

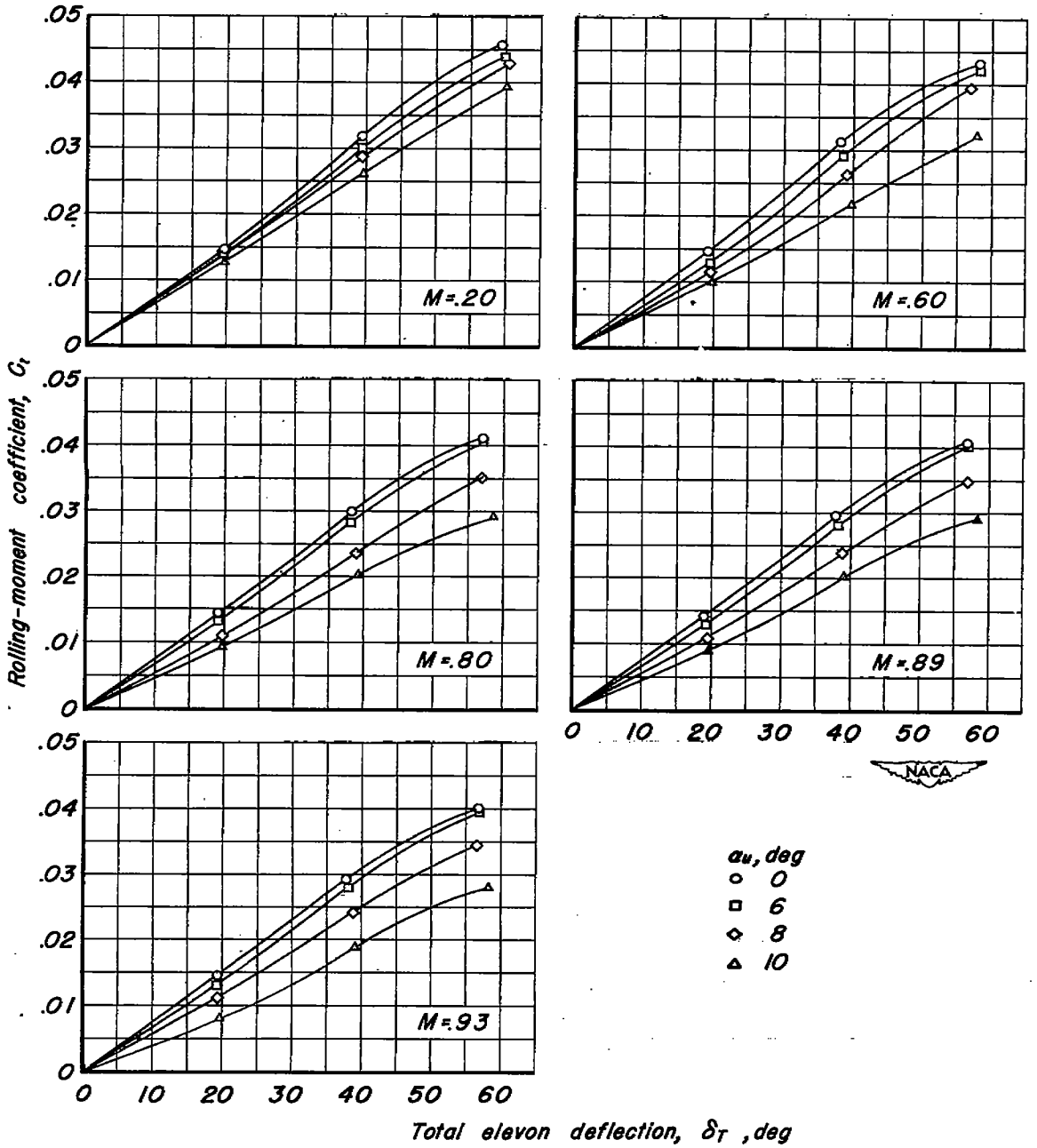

Figure 13.- The variation of rolling-moment coefficient with total elevon deflection at various angles of attack for several Mach numbers.

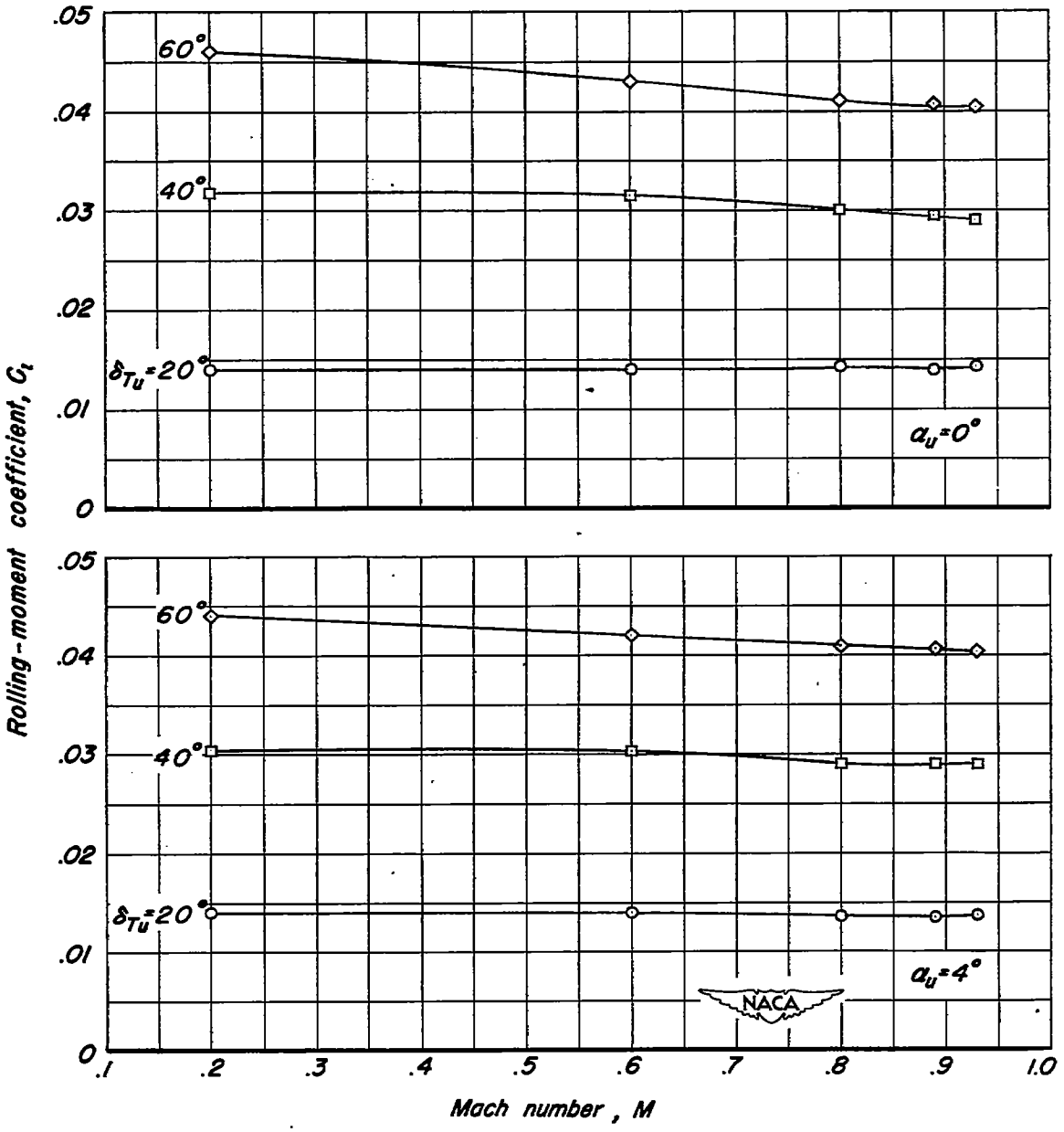

Figure 14.- The effect of Mach number on the rolling-moment effectiveness of the elevons.

[redacted]

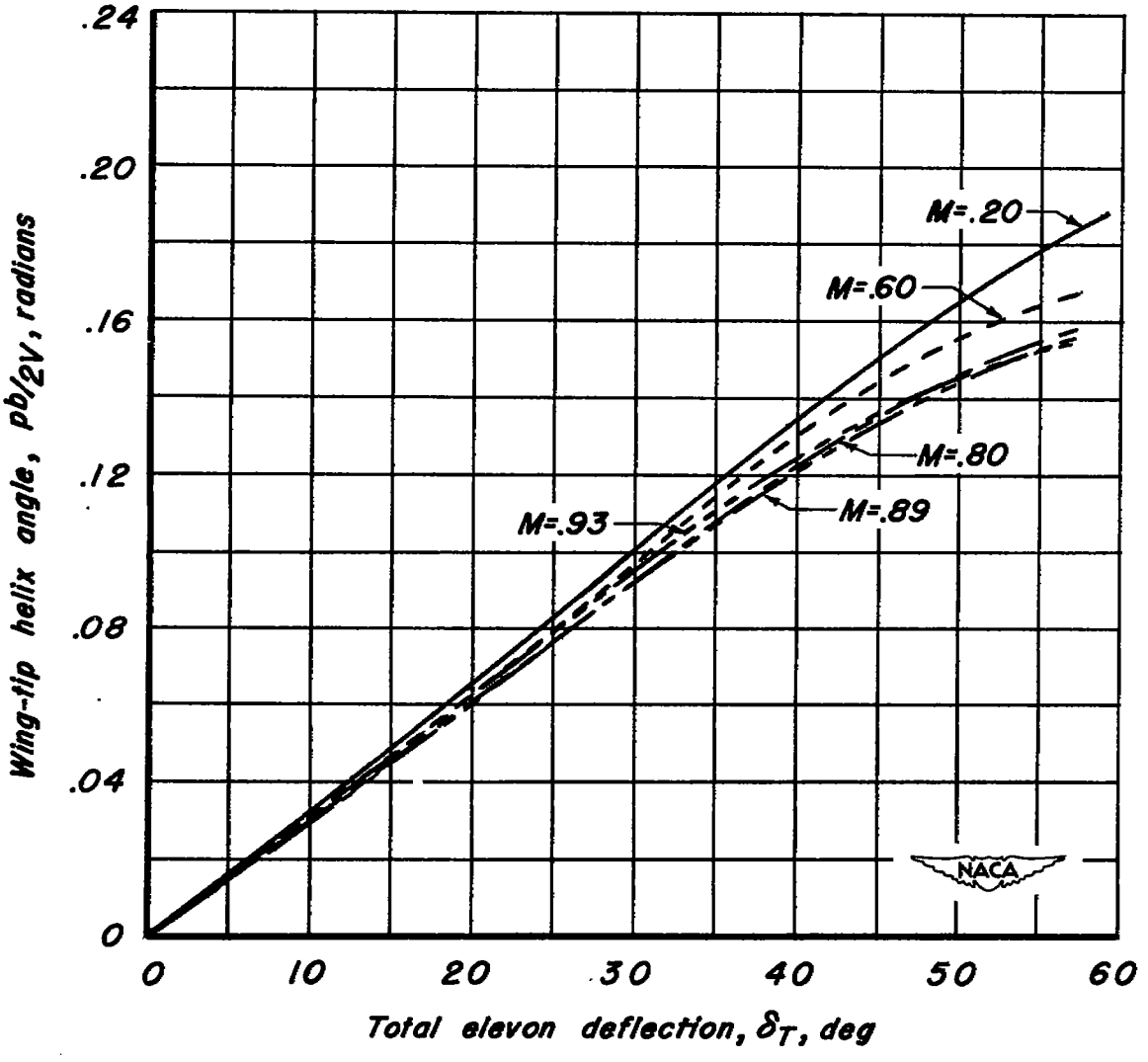

Figure 15.- The variation of the wing-tip helix angle with total elevon deflection for several Mach numbers at a lift coefficient of 0.20.

[redacted]

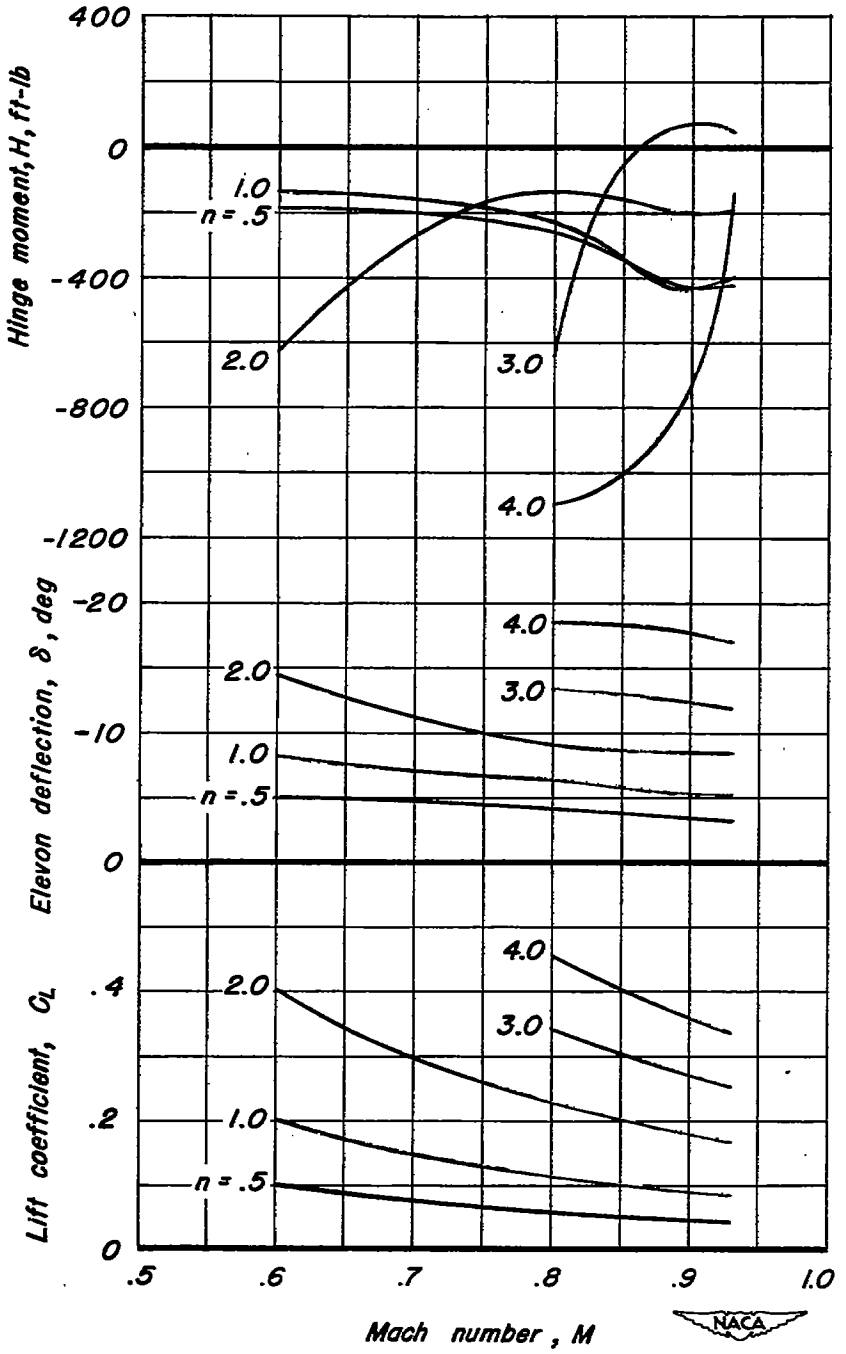

Figure 16.- The variation with Mach number of hinge moment, of elevon deflection, and of lift coefficient for several normal acceleration factors of a tailless airplane at 25,000 feet altitude. Wing loading, 40 pounds per square foot; wing area, 714.3 square feet; center of gravity at 0.25$\bar{c}$.

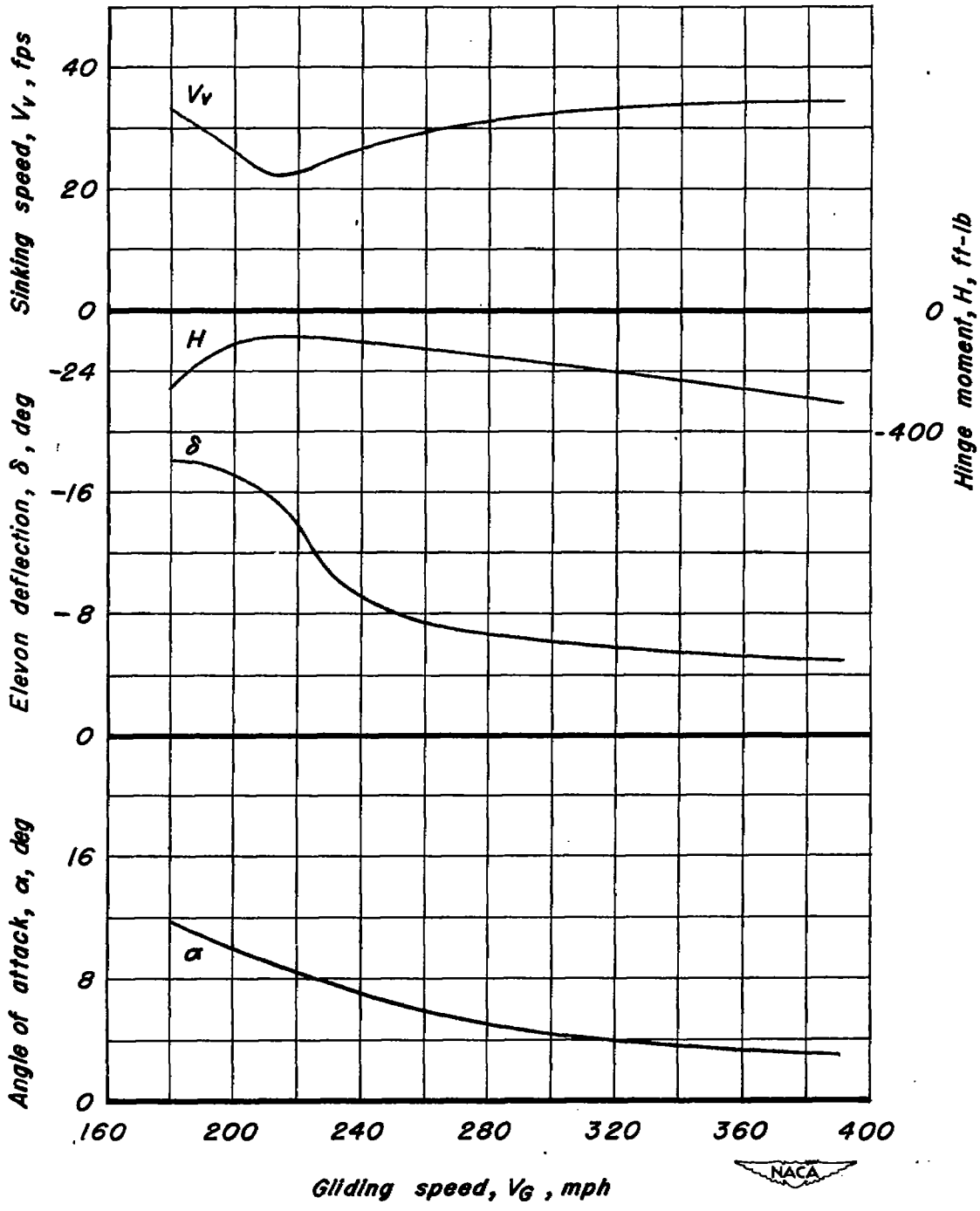

Figure 17.- The variation with gliding speed of sinking speed, hinge moment, elevon deflection, and angle of attack for a tailless airplane at sea level. Wing loading, 40 pounds per square foot; center of gravity at 0.25c̄.

[redacted]